Cellular responses to combined irradiation with alpha particles and X-rays

Alice Sollazzo

Academic dissertation for the Degree of Doctor of Philosophy in Molecular Bioscience at Stockholm University to be publicly defended on Wednesday 27 September 2017 at 10.00 in Vivi Täckholmsalen (Q-salen), NPQ-huset, Svante Arrhenius väg 20.

Abstract

Mixed radiation fields, where different ionizing particles act together, are very important in radiobiology and in radiation protection. Mixed beams are not only the most common form of radiation exposure, but the prediction of their biological effect is also full of uncertainties. Currently, prediction of the biological damage of exposure to mixed radiation fields is based on the default assumption of simple additivity between the effects of all the radiation in the field. This assumption has been proven to be incorrect. Indeed, the simultaneous effect of different radiation qualities has been shown to be greater than additive, namely synergistic. This implicates that, for instance, the predicted cancer risk for astronauts, that remain a prolonged time in space, is currently underestimated as well as the risk of developing secondary cancer for radiotherapy patients.

This thesis aims at understanding the mechanisms behind the cellular response to simultaneous exposure to alpha particles and X-rays (that is referred as mixed beam).

Paper I describes the cell killing and the mutagenic effect of mixed beam exposure in human lymphoblastoid wild type and in cells with impaired capacity to repair oxidative DNA damage .We found that oxidative DNA damage plays an important role in the lethal, synergistic effect of mixed beams.

Paper II and III investigates whether mixed beams exposure leads to an augmented DNA double strand breaks (DSB) induction or to an altered response of the cellular DSB repair machinery. We found that mixed irradiation resulted in synergistic induction of DSB, and that those lesions were repaired with slow kinetics.

Paper IV focuses on the effect of mixed beams at the level of DNA damage in normal cells. Induction and repair of DNA lesions such as DSB, single strand breaks and apurinic sites was quantified using the alkaline comet assay. We found that alpha particles and X-rays interacted in inducing DNA damage. Moreover, although mixed beam exposure resulted in strong activation of the DNA damage response, it resulted in delayed repair.

Although more research is needed to fully elucidate the mechanisms behind the detected synergistic effects, our results strongly suggest that an overwhelmed DNA-repair system causes delay in repair of damage.

Keywords: *Radiation, DNA damage, mutations, alpha particles, X-rays, mixed beam.*

Stockholm 2017
http://urn.kb.se/resolve?urn=urn:nbn:se:su:diva-145509

ISBN 978-91-7649-887-3
ISBN 978-91-7649-888-0

Department of Molecular Biosciences, The Wenner-Gren Institute

Stockholm University, 106 91 Stockholm

CELLULAR RESPONSES TO COMBINED IRRADIATION WITH ALPHA PARTICLES AND X-RAYS

Alice Sollazzo

Stockholm University

Cellular responses to combined irradiation with alpha particles and X-rays

Alice Sollazzo

©Alice Sollazzo, Stockholm University 2017

ISBN print 978-91-7649-887-3
ISBN PDF 978-91-7649-888-0

Printed in Sweden by Universitetsservice US-AB, Stockholm 2017
Department of Molecular Biosciences, The Wenner-Gren Institute

To my father...

Sammanfattning

Hur skadlig är blandad strålning?

De flesta människor förknippar joniserande strålning och radioaktivitet med något negativt, cancerframkallande och allmänt livshotande. Men strålning är en del av våra liv. Vi blir exponerade för små doser strålning som kommer från rymden, från maten vi äter, och luften i form av radongas. Dessutom är det ett oerhört viktigt verktyg inom medicin (t.ex. röntgen, cancerterapi) och industri (sterilisering av maten, energiproduktion). Höga strålningsdoser är skadliga för oss och alla levande organismer. De frigör hög energi i ett mycket begränsat område och kan därför bryta sönder DNA-molekylen och ge upphov till dubbelsträngsbrott (DSB). DSB sker när båda DNA-strängarna klipps sönder. DSB är den mest dramatiska skada som kan uppkomma i DNA:t och, om inte de repareras omgående, kan de ge upphov till genetiska mutationer, genomisk instabilitet och cancer.

Inte all strålning är lika skadlig. Tätjoniserande strålning, som alfapartiklar och tunga joner, består av relativt stora partiklar som levererar mycket energi längs deras bana. De har hög biologisk effekt eftersom de orsakar komplexa skador som är mycket svåra att reparera. Glesjoniserande strålning, som röntgen- och gammastrålning, levererar sin energi jämnt fördelad i små energikvanta (energipaket). De resulterade skadorna på DNA:t är enklare för organismerna att reparera. Blandad strålning är när flera olika stråltyper finns närvarande samtidigt. Detta sker vid t.ex. strålterapi och flyg- och rymdresor.

Medan effekterna av tät- och glesjoniserande strålning är väl dokumenterade, är den biologiska effekten av blandad strålning endast baserad på teoretiska beräkningar. För närvarande antas det i beräkningen att olika stråltyper inte interagerar med varandra. Därför kan deras individuella effekter adderas på ett enkelt, additivt sätt:

$$Effekt\ (bladad\ strålning) = Effekt\ (stråltyp\ a) + Effekt\ (stråltyp\ b)$$

Problemet är att detta antagande har visats vara inkorrekt i flera studier. Effekten av blandad strålning visade sig vara större än additiv, nämligen synergistisk:

$$Effekt\ (bladad\ strålning) > Effekt\ (stråltyp\ a) + Effekt\ (stråltyp\ b)$$

Detta innebär t.ex. att risken för cancerpatienter att utveckla sekundär cancer som följd av strålterapi kan för närvarande vara underskattad.

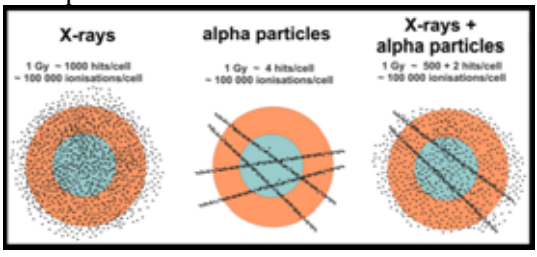

Figur 1: Schematisk bild av en cell bestrålad med glesjoniserande strålning (X-rays), tätjoniserande strålning (alpha particles) och blandad strålning (X-rays + alpha particles)

Denna avhandling undersöker följande frågor:

-Hur reagerar humana celler när de blir träffade av blandad strålning av alfapartiklar och röntgenstrålning.
-Vilka mekanismer ligger bakom den synergistiska effekten?

Artikel I undersöker överlevnad och mutationer i humana celler som exponerats för blandad strålning av alfapartiklar och röntgenstrålning. Dessutom undersöktes rollen av strålningsinducerade fria radikaler. Våra resultat visade att blandad strålning var mycket skadlig och minskade överlevnad av humana celler på ett synergistiskt sätt. Våra resultat tydde också på att den synergistiska effekten var orsakad av strålningsinducerade fria radikaler. Ingen effekt kunde detekteras på mutationsnivå.

Den andra och tredje artikeln fokuserade på dubbelsträngsbrott (DSB), där båda DNA-strängarna gått av. För att sätta ihop DNA-strängarna igen behöver cellerna lokalisera skadan. Reparation av DSB börjar med att ett signalprotein som kallas 53BP1 ansamlas nära DNA-skadan. Detta protein fungerar som en flagga som signalerar dessa allvarliga skador. Ansamlingen kan direkt ses i fluorescensmikroskop som lysande prickar (foci). Antalet foci av signalprotein kan användas som mått på hur många strängbrott som bildades efter bestrålning. Minskningen i antalet över tiden kan indikera lyckat lagning av DNA-strängar.

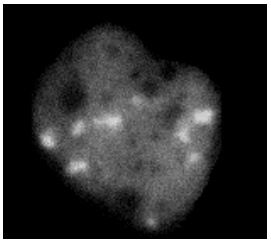

Figur 2: En cellkärna efter alfa strålning. Lysande prickar (foci) är ansamlingar av signalprotein som markerar där båda DNA-strängarna gått av.

I **artikel II** analyserades foci i icke-levande (fixerade) bencancerceller. Antalet foci som bildades efter blandad strålning var större än förväntat om man antog att effekten mellan alfapartiklar och röntgenstrålning var additiv. Den synergistiska effekten kunde också detekteras genom att studera reparationskinetik för DSB. Foci som bildades efter blandad strålning reparerades mycket långsamt. Resultat tyder på att alfapartiklar och röntgenstrålning interagerar med varandra och genererar skador i DNA:t på ett synergistiskt sätt. Till följd av detta blir cellernas reparationssystem mättat vilket gör att skadorna lagas långsamt.

Artikel III fokuserade på dynamiken av 53BP1 foci i levande cancerceller. Cellerna filmades under 75 minuter efter bestrålning och foci analyserades. Filmerna visade att cellkärnan är en dynamisk struktur. Foci bildades och reparerades hela tiden. De foci som genererades av blandad strålning var mer begränsade i sina rörelser än de foci som bildades efter endast alfapartiklar eller röntgenstrålning. Vad denna skillnad berodde på var oklart. Dessa foci hade dessutom högst koncentration av signalproteinet vilket tyder på att skadorna signalerade starkt. Trots stark signalering kunde skadorna inte repareras under filmtiden. Resultatet indikerar att DNA-skador som orsakas av blandad strålning är svåra för cellen att reparera.

I **artikel IV** undersöktes olika typer av DNA-skador i blodceller efter bestrålning. Dessutom analyserades aktivering av den cellulära responsen på DNA-skador. Resultaten bekräftar att blandad strålning orsakar mer skada än vad som kan beräknas från additiva effekter av de olika stråltyperna. Detta leder till oerhört stark aktivering av den cellulära responsen efter DNA-skada.

Sammanlagt tyder de resultat som presenteras i denna avhandling på att den nuvarande metoden för att beräkna den biologiska effekten av blandad strålning borde revideras. DNA-skadan som orsakas av blandad strålning av alfapartiklar och röntgenstrålning sker på inte på ett additivt sätt utan synergistiskt. Skadorna leder till stark aktivering av de cellulära reparationsprocesserna, men dessa blir överbelastade och skadorna repareras med långsam kinetik.

List of publications

This thesis is based on the following papers:

I. **Sollazzo, A**., Shakeri-Manesh, S., Fotouhi, A., Czub, J., Haghdoost, S. & Wojcik, A. 2016, "Interaction of low and high LET radiation in TK6 cells—mechanistic aspects and significance for radiation protection", *Journal of Radiological Protection,* vol. 36, no. 4, pp. 721.

II. **Sollazzo, A**., Brzozowska, B., Cheng, L., Lundholm, L., Haghdoost, S., Scherthan, H. & Wojcik, A. "Alpha particles and X-rays interact in inducing DNA damage in U2OS cells", *Accepted for publication in Radiation Research.*

III. **Sollazzo, A**., Brzozowska, B., Cheng, L., Lundholm, L., Scherthan, H. & Wojcik, A. Live dynamics of 53BP1 DNA damage foci induced by a combination of clustered and dispersed double strand breaks. *Manuscript.*

IV. Cheng, L., Brzozowska, B., **Sollazzo, A**., Lundholm, L., Lisowska, H., Haghdoost, S., Wojcik, A. Comet assay reveals an interaction of DNA lesions and impairment of DNA repair in peripheral blood lymphocytes simultaneously exposed to alpha particles and X-rays. *Manuscript.*

Contributions to the papers

Paper I: The founding for was granted by SSM to my supervisor. The cellular models used in the experiments were provided by Dr. Haghdoost at Stockholm University. I designed the experimental setup and performed the experimental work described in the papers. I took part in the data analysis and contributed to the writing of the paper. Moreover, the hypothesis of disruption of high-order chromatin structure and the role of oxidative damage in the detrimental effect of mixed beam irradiation was conceived by me.

Paper II and III: The project was conceived by my supervisor, the founding was partly granted by SSM. The cellular models used in the experiments were donated by Dr. Lukas from Danish Cancer Society, Copenhagen. I designed the experimental setup and performed the experimental work described in both papers. In **Paper II**, image-analysis of fixed cells was performed by me using a macro written for ImageJ by Beata Brzozowska from Department of Biomedical Physics, Faculty of Physics, University of Warsaw, Poland. I took part in the data analysis and in the writing of the manuscript. **Paper III**: the microscope used for live cell imaging was provided by H. Scherthan (Scherthan and Adelfalk, 2011). The macro for live-cell imaging analysis was written by me using the image-processing package "Fiji". The idea of measuring the movements of damaged chromatin was suggested by me. Moreover, due to the amount of data acquired with Fiji, I had to learn "R" programming language to analyze the data. I performed the vast majority of the data analysis and I took part in manuscript writing.

Paper IV: My contribution in has been mainly into the development and troubleshooting of the comet assay, carrying out preparatory experiments and interpretation of the results.

Papers not included in this thesis

- Brzozowska, B., **Sollazzo, A**., Cheng, L., Lundholm, L. & Wojcik, A. 2016, "EP-2072: Spatiotemporal dynamics of DNA damage in cells exposed to mixed beams of ionising radiation", *Radiotherapy and Oncology,* vol. 119, pp. S977-S978.
- Cheng, L., Lisowska, H., **Sollazzo, A**., Wegierek-Ciuk, A., Stepień, K., Kuszewski, T., Lankoff, A., Haghdoost, S. & Wojcik, A. 2015, "Modulation of radiation-induced cytogenetic damage in human peripheral blood lymphocytes by hypothermia", *Mutation Research/Genetic Toxicology and Environmental Mutagenesis,* vol. 793, pp. 96-100.
- Dang, L., Lisowska, H., Manesh, S.S., **Sollazzo, A**., Deperas-Kaminska, M., Staaf, E., Haghdoost, S., Brehwens, K. & Wojcik, A. 2012, "Radioprotective effect of hypothermia on cells – a multiparametric approach to delineate the mechanisms", *International journal of radiation biology,* vol. 88, no. 7, pp. 507-514.
- Danielsson, D., Brehwens, K., Halle, M., Marczyk, M., **Sollazzo, A**., Polanska, J., Munck–Wikland, E., Wojcik, A. & Haghdoost, S. 2016, "Influence of genetic background and oxidative stress response on risk of mandibular osteoradionecrosis after radiotherapy of head and neck cancer", *Head & neck,* vol. 38, no. 3, pp. 387-393.
- Sibony, D., Horowitz, Y.S., Oster, L., Wojcik, A. & **Sollazzo, A**. 2014, "Combined measurement of dose and α/γ radiation-field-components using the shape of composite peak 5 in the glow curve of LiF:Mg,Ti", *Radiation Measurements,* vol. 71, pp. 86-89.
- Sun, J., Lou, X., Wang, H., **Sollazzo, A**., Harms-Ringdahl, M., Skog, S., He, E. & Haghdoost, S. 2015, "Serum 8-hydroxy-2-deoxyguanosine (8-oxo-dG) levels are elevated in diabetes patients", *International Journal of Diabetes in Developing Countries,* vol. 35, no. 3, pp. 368-373.
- Acheva, A., Haghdoost, S., **Sollazzo, A**., Launonen, V., Kämäräinen., M. Presence of stromal cells enhances epithelial-to-mesenchymal transition (EMT) induction in lung bronchial epithelium after protracted exposure to gamma radiation". *Submitted manuscript*

Contents

List of abbreviations

AP-site	Apurinic/apyrimidinic, also called abasic site
ARF	ADP-ribosylation factor
ATM	Ataxia Telangiectasia Mutated
ATP	Adenosine-triphosphate
ATR	Ataxia Telangiectasia and Rad3 Related
BER	Base excision repair
Bp	Base pair
BRCA1	Breast cancer 1
BRCA2	Breast cancer 2
53BP1	Tumor suppressor p53-binding protein 1
CDC25A	Cyclin-dependent kinase 25A
CHO cells	Chinese hamster ovarian cells
Chk2	Checkpoint kinase 2
CRAN	Comprehensive R Archive Network
CSR	Immunoglobulin class switch recombination
CTIP	C-terminal binding protein 1 interacting protein
DNA-PKcs	DNA-dependent protein kinase catalytic subunit
DSB	Double Strand Break
GFP	Green fluorescent protein
Gy	Grey, Unit of absorbed energy = J/kg
HEPES	4-(2-hydroxyethyl)-1-piperazineethanesulfonic acid
HIV	Human immunodeficiency virus
hMYH	Human MutY homolog protein
hOGG1	Human MutM homolog protein
HR	Homologous recombination
H2A(X) k15Ub	Ubiquitinated form of H2AX
H3	Histone 3
H3K9me3	Trimethylated lysine 9 of histone 3
IR	Ionizing radiation
IRIF	Ionizing radiation induced foci
Ku70/Ku80	Lupus Ku autoantigen protein p70/p80
LET	Linear energy transfer
LF	Large foci
LINC complex	Linker of the nucleoskeleton and cytoskeleton
MDC1	Mediator of DNA damage checkpoint 1
MDM2	Mouse double minute 2 homolog
MDM4	Mouse double minute 4 homolog
MRN	Mre11-Rad50-NSB1 complex

MSD	Mean Squared Displacement
MYH	see hMYH
NHEJ	Non-homologous end joining
OGG1	see hOGG1
8-oxo-dG	8-oxo-7,8,dihydroxy-2´-deoxyguanosine
p-ATM	Phosphorylated ATM
PARP	Poly (ADP-ribose) polymerase
PE	Plating efficiency
PEST	Penicillin Streptomycin
Pol	Polymerase
p.r.	Post irradiation
p21	Cyclin-dependent kinase inhibitor
p53	Protein 53
p-p53	Phosphorylated p53
RAD51	Radiation sensitive 51
RAD54	Radiation sensitive 54
RBE	Relative biological effectiveness
RNF168	RING domain-containing protein 168
RNF8	RING domain-containing protein 8
ROS	Reactive oxygen species
RPA	Replication protein A
RTI	Relative tail intensity
SF	Small foci
SSB	Single strand breaks
TFT	Trifluorthymidine
TK	Thymidine kinase
TK6	Thymidine kinase heterozygote cell line
$TK6^{WT}$	TK6 wild type
$TK6^{MYH-}$	TK6 with reduced expression of MYH
TOPB1	Topoisomerase II-binding protein 1
TTP	Thymidine triphosphate
UBC13	Ubiquitin E3 ligase complex
UBA1	Ubiquitin-activating enzyme
dUMP	Deoxy uracil monophosphate
USP28	Ubiquitin specific protease
U2OS	Human Osteosarcoma cells
WR	Radiation weighting factor
XLF	XRCC4-like factor
XRCC4	X-ray repair cross-complementing

Introduction

Different types of radiation

Radiation is defined as "the emission and propagation of energy through matter or space as electromagnetic waves or as moving subatomic particles" (Hall and Giaccia 2012b). It is usually classified into ionizing and non-ionizing radiation. This thesis focuses on ionizing radiation (IR or just radiation in the following text). IR is described as waves or particles that have enough energy to remove electrons from atoms and molecules. In contrast, non-ionizing radiation carries a lower amount of energy per quantum and it can only move electrons to higher energy levels (excitation) (Joiner and vand der Kogel 2009). Non-IR will not be further discussed in this thesis.

When IR is absorbed in cells and tissues, it delivers a high amount of energy in a confined space. The energy released per ionizing event is about 33 eV and it can easily break a strong chemical bond. However, the total energy delivered by IR is relatively small. For example, a whole-body exposure to 4 Gy is lethal to humans but it corresponds to the energy absorbed by drinking one sip of a hot beverage (Hall and Giaccia 2012b).

IR may be described as electromagnetic radiation such as X- and gamma rays or particulate radiation as alpha and beta particles, neutrons, protons and heavy ions (Joiner and vand der Kogel 2009). This thesis focuses on the effect of X-rays and alpha particles, therefore the other types of IR will not be described in more details. Sometimes, the term X- or gamma rays is interchanged. Both rays are photons and therefore they share the same properties (Hall and Giaccia 2012b). However, they differ in the way how they are produced. X-rays are generated in an electrical device called Crookes tube in the form of bremsstrahlung while gamma rays are emitted by the nuclei of radioactive isotopes. In the Crookes tube, electrons are first accelerated to high energy and then stopped abruptly in a target. Due to the deceleration, part of the kinetic energy is emitted as photons (X-rays). Gamma rays are emitted when radioactive nuclei decay into more stable forms. Exemplary sources of gamma rays are Potassium-40 (^{40}K), Cesium-137 (^{137}Cs) and Cobalt-60 (^{60}Co) (McNair, Glover, Wilson 1956; Meisberger, Keller, Shalek 1968). The energy

of X- and gamma rays is equal to *hv*, where *h* is Planck's constant and v is the frequency (Hall and Giaccia 2012b). The photons are uncharged and, therefore, they can travel several centimeters in water and long distances in air, whereas they are efficiently stopped by lead (Martin and Sutton 2015).
Alpha particles are helium nuclei (two neutrons and two protons) which are naturally produced during alpha decay of radioactive nuclides such as uranium or radium. Radium-226 decays to radon-222 with the emission of an alpha particle while uranium-238 becomes uranium-234 with a similar process (Hall and Giaccia 2012b). Alpha particles are positively charged and they can be easily accelerated in particle accelerators or in cyclotron waves in the solar winds (Barbui et al. 2015; Brobeck et al. 1947). Depending on the particle energy and the medium traversed, alpha particles can travel as far as 0.1 mm in H_2O or up to 4 cm in air and they are efficiently stopped by a sheet of paper (Francis et al. 2011). The energy deposition of alpha radiation and other massively charged particles during their travel through matter is described by the Bragg curve. This curve has a well-defined peak of energy deposition at the end of the particle track. For an alpha particle travelling through a tissue, the majority of ionization events occur immediately before the particle stops (Hall and Giaccia 2012b). The shape of the Bragg curve is used in modern proton cancer therapy (Karger and Oliver 2007).

RBE and LET

Ionizing radiation can be described using different parameters. The absorbed dose (D) is the physical quantity that describes the amount of energy absorbed by matter after radiation exposure. However, equal doses of different types of radiation do not produce equal biological effect. The equivalent dose (H_T) describes the biological effect of radiation on tissues and living organisms taking into consideration both the absorbed dose (D) and the radiation quality (W_R). The absorbed dose is measured in Gray, Gy, where 1Gy = 1J/kg while the equivalent dose in measured in Sievert, Sv (Joiner and vand der Kogel 2009). An important parameter often used in dosimetry is the linear energy transfer (LET), which describes the energy transferred by the ionizing particle to matter as a function of track distance. The unit of LET is kiloelectron volt per micrometer, keV/ μm (Hall and Giaccia 2012b). It should be considered that LET is an average value, and therefore it has limitations. Additionally, LET

can be calculated in different ways, namely as track average, or energy average. The track average is calculated by dividing the track into equal lengths and the energy deposited in each length is averaged. In contrast, in the energy average, the track is divided into equal energy intervals and the lengths of the intervals are averaged (Hall and Giaccia 2012b). In general, high LET values implicate that the particles deliver high amount of energy in a short distance. As a consequence, high LET particles induce strong biological effects but they have limited penetrating power. High LET radiation, such as alpha particles and heavy ions are densely ionizing, with the majority of ionization occurring along the track of the charged particle (Hill 1999). This implicates that, in a cellular system, a single alpha particle may induce on average about - 200 SSB and ~ 20 DSB all of them confined in close proximity of the particle track (Goodhead 1995). The damage induced is highly clustered. In contrast, low LET radiation such as X- and γ-rays are sparsely ionizing (Ward 1994). Here, a single particle in typical cell nucleus will on average create ~ 1 SSB and - 0.04 DSB (Goodhead 1992). The resulting lesions are less clustered and easier for a cell to handle (Goodhead, Thacker, Cox 1993).

Equal doses of different types of radiation do not produce equal effects on tissues and organisms. The relative biological effectiveness (RBE) is used when comparing the biological effect of exposure to different radiation qualities (Hall and Giaccia 2012b). Given the same radiation dose, RBE is calculated as the "ratio of physical doses between two different types of radiation required to produce the same biological endpoint" (Laramore et al. 2013). The dose of 250 kV X-rays is used as the standard (Hall and Giaccia 2012b). RBE increases with LET to a maximum at about 100 keV/ μm, thereafter it decreases due to overkilling effect (Barendsen et al. 1963). RBE is dependent on several factors such as the radiation dose (D), radiation quality (LET), dose rate, number of dose fractions, biological system or endpoint (Hill 1999). Although, it is general consensus that the RBE is highly dependent on the above mentioned factors, meta-analysis studies on radiation induced cell-killing propose that LET alone can be an adequate parameter for describing RBE(Sørensen, Overgaard, Bassler 2011).

DNA and chromatin

To fit into such a small volume, DNA is packed into a condensed structure, with a strict hierarchical organization, the chromatin (Lebeaupin et al. 2015). The primary building block is the nucleosome, a 10 nm in diameter structure, made of an octameric histone core with about 147 bp of DNA wrapped around it. The octameric core consists of two copies each of the histones (H2A, H2B, H3 and H4) (Lodish et al. 2000). The N-terminal tails of the histones extend out from the core and can be modified by acetylation, methylation, or ubiquitination (Eberharter and Becker 2002; Wang et al. 2004; Zhang and Reinberg 2001). The secondary structure of the chromatin is built up by chromatin loops of variable size ranging from few kilobases to several megabases (Rao et al. 2014). Condensed chromatin, the heterochromatin, is thought to indicate transcriptionally inactive regions of DNA (Brown et al. 1997; Grewal and Moazed 2003). In contrast, transcriptionally active domains are characterized by a more open structure, namely the euchromatin (Lodish et al. 2000). Chromatin condensation can be modulated by post- translational modification of histone molecules. Generally, acetylation/deacetylation of lysine on the N-termini of the histones controls how tightly the DNA is bound to the histone core (Shogren-Knaak et al. 2006).

Figure 1: Schematic representation of DNA packed in chromatin fibers. Modified from (Lodish et al. 2000).

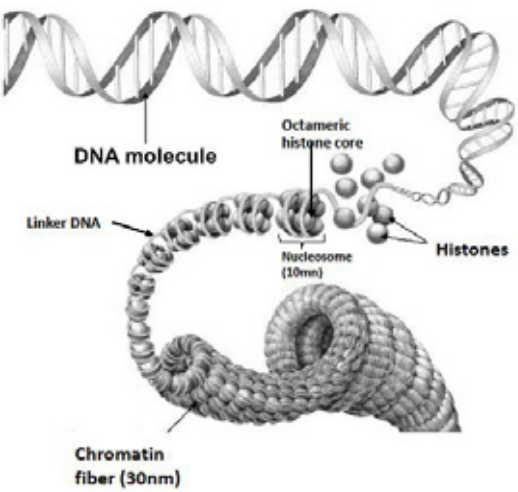

While hyper-acetylation induces relaxation of chromatin, deacetylation tights the DNA to the histone octamer (Eberharter and Becker 2002). Other histone

modifications include methylation and ubiquitination. Methylated histones can be found in heterochromatic regions such as methylation on histone H3 lysine 9 (H3K9) or in actively transcribed domains (H3K4 methylation) (Shilatifard 2008). RNF8- dependent ubiquitination on histone H2AX may be found at the site of chromatin damage (Huen et al. 2007).

Finally, the ternary structuring level of the chromatin refers to the spatial distribution of the chromosome territories in the nucleus (Lieberman-Aiden et al. 2009). Chromosome domains are positioned non-randomly and their location in the nucleus is maintained by interactions with the inner nuclear membrane (Kinney, Onufriev, Sharakhov 2015).

Recently, the 3D structure of the mammalian genome has been identified showing the intricate folding of chromosomes domains inside the nucleus (Stevens et al. 2017).

Chromatin movements

The chromatin is a highly dynamic structure. Beside histone replacements and shift in nucleosome positioning, a number of papers have detected physical movements of the chromatin fiber itself (Aten et al. 2004; Becker et al. 2014; Bornfleth et al. 1999; Campos and Reinberg 2009; Lottersberger et al. 2015; Segal and Widom 2009).

Several studies calculated that intact genomic loci move with a diffusion coefficient ranging from 10^{-4} to $10^{-3}\mu m^2/s$ regardless of the species studied, the range of the nuclear size, or the method of tracking (Chubb et al. 2002; Heun et al. 2001; Neumann et al. 2012; Weber, Spakowitz, Theriot 2010a). It was found that movements of intact chromatin can be described by random walk in a constrained space (Marshall et al. 1997). This result was confirmed in yeast, in bacteria and in mammalian cells (Bornfleth et al. 1999; Jakob, Splinter, Taucher-Scholz 2009; Neumann et al. 2012; Weber, Spakowitz, Theriot 2010b; Weber, Spakowitz, Theriot 2012). It has been proposed that physical constrains to free chromatin movement come from the intrinsic viscosity of the nucleoplasm, anchorage to the nuclear structure and interaction with DNA binding proteins (Cabal et al. 2006; Chubb et al. 2002; Dion and Gasser 2013; Weber, Spakowitz, Theriot 2010b). Thus, the current idea is that intact chromatin in interphase nuclei exhibits a random walk in a confined space with movements ranging from 0.3 to 1 μm (Lebeaupin et al. 2015).

Chromatin mobility during DNA repair

More recent research has focused on DNA mobility after DSB induction. While intact, non-transcribing chromatin behaves in a similar way in all model organisms studied, the dynamics of damaged DNA differs largely in yeast and mammals. In yeast, the induction of a DSB increases the mobility of both the damaged and undamaged loci (Miné-Hattab and Rothstein 2012; Sonoda et al. 2006) This overall increased in chromatin mobility could not be observed in haploid cells and during resection, suggesting that it may be generated by homology searching processes (Saad et al. 2014; Seeber, Dion, Gasser 2013).
Research on mammalian cells gave inconclusive results. Kruhlak et al., (2006) show that chromatin elicit limited mobility upon DSB induction. However, an ATP-dependent decondensation of chromatin in proximity of the break was detected, which possibly facilitates the access of DDR proteins (Jakob et al. 2011; Kruhlak et al. 2006a). Radiation induced DSB in human osteosarcoma cells, U2OS, show slow mobility with a mean square displacement of ≈0.6 $\mu m^2/h$, which was independent of the radiation quality used to generate the breaks (Jakob et al. 2009). Tracks of IRIF of γ-H2AX , RPA and 53BP1 were clearly identifiable in cells that were fixed up to 10 hours after irradiation with uranium ions (3.0 MeV/nucleon; LET 14,300 keV/μm) and low energy carbon ions (9.5 MeV/nucleon; LET 200 keV/ μm). The persistence of particle tracks suggests restricted mobility of damaged sites (Jakob, Splinter, Taucher-Scholz 2009). However, an increasing number of results suggest that DNA damage increases chromatin mobility. Uncapped telomeres, which can be regarded as DSB, display increased mobility with a diffusion coefficient of 3.7 nm^2/s (measured over a time lapse of 10 min). Their mobility was shown to be dependent on functional microtubule, on 53BP1 protein and on the LINC complex (Lottersberger et al. 2015). Radiation induced DSB that are formed in heterochromatin relocates to euchromatin to be processed (Jakob et al. 2011). Moreover, DSB movements are dependent on the presence of ATM protein (Becker et al. 2014). Moreover, Aten et al., observed changes in morphology of tracks of alpha particles, suggesting a large-scale displacement of the broken DNA ends (Aten et al. 2004). Finally, as seen in yeast, the formation of occasional clustering (contact or fusion) of radiation-induced foci was also observed in mammalian cells (Chiolo et al. 2013; Falk et al. 2007; Jakob et al. 2009; Neumaier et al. 2012). In summary, while several studies report positional stability of damaged DNA domains, the majority of researchers detected increased mobility of chromatin after DSB induction.
The biological function of motion of broken DNA ends is currently under discussion (Hlatky 2012; Seeber and Gasser 2017). Subdiffusion–type random

walk, measured by recording the distance between foci over time, was proposed to facilitate the joining of correct DNA ends after proton and carbon ion irradiation (Girst et al. 2013). If, on the one hand, chromatin mobility may facilitate homology searching of intact DNA template, it may, on the other hand, increase the probability of translocation and chromosomal rearrangements (Falk et al. 2007; Lottersberger et al. 2015). Thus, in order to keep genome integrity, the movements of free DNA ends must be strictly controlled. Hence, it is likely that the DDR and the DSB repair pathway of choice is implicated in regulating the mobility of damaged chromatin.

Genome under constant threat

Biological consequences of DNA damage, repair and mutagenicity

DNA may undergo damage of one sort or another due to both endogenous and exogenous causes. Endogenous factors may be the free radicals produced during normal cellular metabolism, spontaneous deamination of cytosine to uracil and mutations due to errors during DNA replication (De Bont and Van Larebeke 2004; Lindahl 1993; Valko et al. 2007). Additionally, exogenous factors such as alkylating, cross-linking agents and ionizing radiation may cause alterations in the DNA bases (Fu, Calvo, Samson 2012; Hickman and Samson 1999). The major types of DNA damage are abasic sites (AP), base damage (BD), DNA cross-links, single strand breaks (SSB) and double strand breaks (DSB) (Hall and Giaccia 2012a). Because of the constant genomic threat, eukaryotic and prokaryotic organisms have evolved a number of repair mechanisms to cope with the different types of damage. The first line of defense is the chromatin itself (Falk, Lukášová, Kozubek 2008; Kim et al. 2003; Nygren, Ljungman, Ahnström 1995).

Radiation-induced damage

Among all DNA damaging agents, ionizing radiation, IR, is one of the most detrimental ones because it delivers a high amount of energy localized in a confined place (Hall and Giaccia 2012a). Radiation-induced DNA damage can be divided in three categories: base damage (BD), SSB and DSB (Ward 1985). They can be generated directly by radiation or indirectly through the effect of free radicals (Goodhead 1994). In fact, upon IR exposure, water molecules undergo radiolysis producing reactive oxygen species (ROS) such as hydrogen peroxide (H_2O_2), H_2 hydroxyl radicals (•OH) and singlet hydrogen (H•) (von Sonntag 1987). ROS are highly reactive and attack DNA bases with preference for guanine (Halliwell and Gutteridge 2015). However, the detrimental effect of radiation is mainly due to single and double strand breaks with the latter considered the most harmful lesion that a cell can experience (Goodhead 1994). Although the DNA is considered to be the main target, IR may also impair cellular functions by altering protein expression, as shown by the detrimental impact of radiation exposure on the cardiovascular system (Maeda et al. 2017).

Cells respond to DNA damage by activating a complex signaling network that eventually decide cell fate. First of all, DNA damage response (DDR) is activated followed by "decision" between cell survival and death (Ando et al. 2012; Hoeijmakers 2001). Unrepaired DSB may induce permanent cell cycle arrest or programmed cell death (apoptosis). Radiation induced damage cause mutations, chromosomal damage and is involved in genomic instability and cancer induction (Ferguson et al. 2015; Miller and Miller 1981; Roos, Thomas, Kaina 2016).

Radiation-induced complex damage

We usually think about a DSB as a simple cut in the DNA strands with easily ligable 5´-phosphate and 3´hydroxyl. Restriction enzymes produce such simple breaks (Lodish et al. 2000). However, the picture is different after IR exposure. The lesions produced are often referred to as "complex" or "dirty", meaning that the DSBs are surrounded by additional damage such as single strand breaks, apurinic sites and inter-strand crosslinks, among others (Datta, Neumann, Winters 2005; Dextraze et al. 2010; Ravanat et al. 2014; Ward 1994). This phenomenon is defined as clustering of DNA damage: "Two or more lesions formed within one or two helical turns of DNA caused by the passage of a single radiation track" (Ward 1994). Following this definition, a DSB itself can be considered a cluster of two SSB. Researchers have found

that clustered DNA damage may also form endogenously. However, while endogenous oxidative cluster lesions are absent from the genome of DNA repair-proficient cells, they accumulate in the DNA of radiosensitive cell lines (Bennett et al. 2004). Clustering can be divided in two major classes: DSB-related, when DSB are surrounded by other lesions, and non-DSB oxidative clustered DNA lesions, when DSB are not involved (Gollapalle et al. 2007). Quantification of clustered DNA damage has been both predicted using Monte Carlo simulations and verified experimentally in a few cases (Nikitaki et al. 2016a; Nikitaki et al. 2016b). The yield of DSB-related clustered lesions is directly proportional to LET. It has been calculated with Monte Carlo simulations that 70% of the DSB produced after high LET IR are clustered with other DSB while the value drops to 30% after low LET IR. If other DNA damage is taken into consideration, then 90% of the DSB are considered clustered after high LET and 50% after low LET IR (Nikjoo et al. 1999). In the case of non-DSB clusters, the LET dependency is inverted. Monte Carlo simulation as well as in vitro and in vivo studies showed that the yield of oxidative cluster damage decreases with increasing LET (Semenenko and Stewart 2004; Terato et al. 2008). Moreover, Sutherland and colleagues measured that DSB comprise only about 20-30% of all complex DNA damage produced in naked DNA by exposure to X-rays (Sutherland et al. 2000; Sutherland et al. 2001). Moreover, the same authors measured the frequency of different classes of clustered DNA damage in human monocytes after exposure to X-rays at doses below 1 Gy. They found that 28% of clustered damage comprises DSB, a similar percent contains oxidized purine, 25% is made of oxidized pyrimidine, finally 20% contains abasic cluster (Sutherland et al. 2002). More recent studies found that formation of clustered lesions depends on the chromatin packing density (Lorat et al. 2015). However, the frequency of DSB repair foci such as 53BP1 and γ-H2AX per cell decreases with increasing LET (Nikitaki et al. 2016b).

As the frequency of clustering differ between different radiation qualities so does the number of lesions per cluster. Monte Carlo simulations show that there can be up to 25 lesions per cluster after high and 10 after low LET radiation (Semenenko and Stewart 2004). The difference arises because high LET radiations deposit most of their energy into a confined space, causing several direct ionization events in close proximity to each other. Moreover, water radiolysis and the subsequent reactive oxygen species produced, will further cause additional damage in close proximity. In contrast, the random energy deposition by low LET radiation will induce widely spread damage, reducing the probability of clustering (Sutherland et al. 2002).

Cellular response to DNA damage

Repair of clustered oxidative DNA damage

While cells are normally able to repair single lesions in the DNA, multiple damage sites slow down the repair processes (Georgakilas, O'Neill, Stewart 2013). Moreover, if several lesions are located on opposite DNA strands, they may form additional DSB. This is particularly true in yeast and bacteria (Sage and Harrison 2011). In contrast, in mammalian cells the repair processes are more complex with a hierarchy of lesion procession (Eccles, Lomax, O'Neill 2009). Oxidative damage clustered within a strand break will not be processed until the break is cleared. Similarly, a base damage such as 8-oxodA will slow down the repair of an AP site (Lomax et al. 2005). However, the order of repair largely depends on the type of damage. Two apurinic sites have high potential to be converted into a DSB because they are rapidly excised prior to repair. If two AP sites occur on the opposite site of a DNA strand, more than three bases apart, then they are rapidly incised, leading to DSB formation (Paap, Wilson III, Sutherland 2008). It was estimated that around 10% of non-DSB clusters generated by low LET radiation is converted into DSB within 30 minutes from exposure (Gulston et al. 2004). Finally, overexpression of the DNA glycosylase hOGG1 increases the yield of DSB formed after irradiation, showing that repair of oxidized guanine may generate additional breaks (Yang, Galick, Wallace 2004). Clustering is currently believed to be the main factor accountable for the genotoxicity of radiation and other radiomimetic drugs such as Bleomycin and Neocarzinostatin (Povirk and Finley Austin 1991; Regulus et al. 2007). In summary, what makes radiation so harmful to cells and organisms is the clustering of DNA damage that slow down the processing of lesions leading to incomplete or incorrect repair.

Base damage: repair of oxidized guanine

The mechanism responsible for correcting base damage is the base excision repair, BER. BER can both remove single nucleotides (short patch BER) or it can replace up to 10 nucleotides at the same time (long patch BER). In general, BER is initiated by DNA glycosylases that catalyze the hydrolysis of N-glycosyl bonds of oxidized bases in the DNA. Thereafter, the oxidized bases are removed either by the DNA glycosylase itself or by an AP endonuclease resulting in an AP-site. Finally, the AP site is repaired by polymerases which insert new complementary nucleotides (Cadet and Davies 2017). Due to the

high redox-potential, oxidized guanine is the most abundant type of oxidative damage generated by IR (Dizdaroglu 1992). When oxidized, it is converted into the guanine adduct 8-oxo-7,8,dihydroxy-2′-deoxyguanosine (8-oxo-dG). If not promptly removed, 8-oxo-dG may mis-pair with adenine, leading to G:C to T:A transversion mutations (Duarte, Muller, Burrows 1999; Moriya and Grollman 1993). Components of BER involved in the removal of 8-oxo-dG in human cells are the glycosylases hOGG1 and hMYH (Radicella et al. 1997; Slupska et al. 1999). While hOGG1 promptly remove oxidized guanine from the DNA, hMYH acts post-replicative by removing adenine when mis-paired with 8-oxo-dG (Robertson et al. 2009; Tsai-Wu, Liu, Lu 1992). Once adenine is removed, DNA polymerase λ can insert cytosine restoring the original sequence (van Loon and Hübscher 2009). However, under high level of oxidative stress, 8-oxo-guanine accumulates and the low fidelity pol β may reintroduce adenine opposite to oxidized guanine (Hashimoto et al. 2004). This futile short patch BER will result in accumulation of hMYH-generated SSB and may lead to programmed cell death (Oka and Nakabeppu 2011).

Processing double strand breaks

DSB can arise both endogenously as a result of collapsed replication forks or meiotic recombination and exogenously as effect of IR and radiomimetic drugs. Regardless of their origin and complexity, DSB are mainly repaired by two enzymatic pathways: classical non-homologous end joining (NHEJ) and homologous recombination (HR) (Jeggo 1998). NHEJ is a rather fast pathway. It is initiated by enzymes that bind to the broken DNA ends. Then, the non-complementary ends are processed and the break is rejoined. In contrast, HR is a slower process. In HR, after the initial cleavage around the 5' DNA end (resection), the single stranded DNA invades the adjacent sister chromatid to find the homologous sequence to use as a template. In contrast to NHEJ, were part of the DNA is lost, HR uses the homologous DNA strand to accurately restore the missing nucleotides. Until recently, it was thought that the DDR involves only enzymatic reactions carried out by proteins. However, recent publications report the presence of RNA molecules in the vicinity of the DNA breaks, suggesting the involvement of RNA in DDR (Hawley et al. 2017). Additionally, there is general consensus that NHEJ is an error-prone mechanism which is active throughout the cell cycle and prevalent in G1, while HR is error-free and mainly active in G2 - S phase (Sonoda et al. 2006). However, the question remains why an error-prone mechanism that allows deletion of DNA is active during the major part of the cell cycle. A recent publication suggested that nascent RNA can be used in NHEJ as a template for replacing the missing nucleotides in actively transcribed genes. The authors showed that RNA polymerase II associates with classical NHEJ proteins such as Ku70/Ku80, DNA-PK, Lig IV among others (Chakraborty et al. 2016). Thus, NHEJ may work error-free in actively transcribed regions of the DNA, where nucleotide depletion would be highly detrimental. Moreover, thanks to its fast kinetics, NHEJ plays a clear role in preserving genomic integrity by suppressing malignant transformation and chromosomal aberrations (Difilippantonio et al. 2000).

Currently, it is not completely understood which factors influence the pathway of choice between NHEJ and HR. The cell cycle stage as well as the interplay between 53BP1 protein and BRCA1 seem to be determinant (Hustedt and Durocher 2017; Isono et al. 2017). While phosphorylated 53BP1 inhibits HR by blocking resection, BRCA1 counteracts NHEJ by promoting 53BP1 dephosphorylation (Chapman, Taylor, Boulton 2012; Isono et al. 2017). Other proteins involved in the choice between NHEJ and HR are: the small GTPase protein, Rif1 and CtIP. Rif1 binds to phosphorylated 53BP1 preventing

BRCA1 accumulation and promoting NHEJ. In contrast, CtIP protein binds to BRCA1 and prevents Rif1 from accumulating, initiating resection (Zimmermann and de Lange 2014). Recently, it has been proposed that 53BP1 and BRCA1 compete for binding to the DNA scaffold protein TOPB1, which is rapidly recruited at the site of DSB (Liu et al. 2017; Ohashi et al. 2014; Shimada and Gasser 2017; Wardlaw, Carr, Oliver 2014). The initial cleavage is poorly understood but it seems to involve MRN and CtIP (Zimmermann and de Lange 2014).

Mechanism of NHEJ

Within seconds after the formation of a DSB, the protein heterodimer Ku70/Ku80 binds to the free DNA ends, functioning as a scaffold for the protein kinase DNA-PK (Gell and Jackson 1999; Mari et al. 2006; Walker, Corpina, Goldberg 2001). DNA-PKcs binds to Ku70/Ku80 form the synaptic complex that holds the free DNA ends together (DeFazio et al. 2002). Once the synaptic complex is built, DNA-PK becomes trans-autophosphorylated, a step that is needed for efficient progression of the NHEJ pathway (Chan et al. 2002). Phosphorylated DNA-PK changes its conformation allowing processing enzymes and ligases to access the synaptic complex (Block et al. 2004). Non-compatible ends can hence be processed either by adding new nucleotides (polymerases) or removing excess ones (Artemis). The endonuclease Artemis becomes activated by phosphorylation and it cleaves the phosphodiester bonds within the polynucleotide chain of the non-complementary strands (Dahm 2007). Once the DNA termini are cleared, they can be ligated together. This is mediated by the ligase IV/ XRCC4 protein complex which is recruited to the synaptic complex by DNA-PK-Ku70/Ku80 (Costantini et al. 2007). Another factor involved in NHEJ, is XLF (Ahnesorg, Smith, Jackson 2006; Buck et al. 2006). Its recruitment depends on ligase IV/ XRCC4 and Ku 70/80 and promotes the ligation of non-compatible DNA ends without nucleotide loss (Gu et al. 2007; Tsai, Kim, Chu 2007).

Mechanisms of HR

HR is initiated by 5´resection which generates 3´single strands (Jasin and Rothstein 2013). Replication protein A, RPA, binds to this structure, competing with Rad51 which is the main protein involved in HR (Krejci et al. 2012). Mediator proteins such as BRCA2 (Rad52 in yeast) displace RPA, allowing Rad51 to form nucleoprotein filaments (Ogawa et al. 1993; Sung 1997). The

filaments are essential for HR progression because they recognize the homologous double stranded DNA (Chen, Yang, Pavletich 2008). Rad51 mediates the physical connection between the invading strand ssDNA and the homologous template forming a D-loop (Petukhova, Stratton, Sung 1998). At this step, Rad51 slowly dissociates from the dsDNA allowing DNA synthesis (Miné et al. 2007). DNA synthesis can take place following different pathways. The most studied is the Double strand break repair model with the formation of Holliday structure and generation of crossover and non-crossover products (Holliday 1964; Szostak et al. 1983).

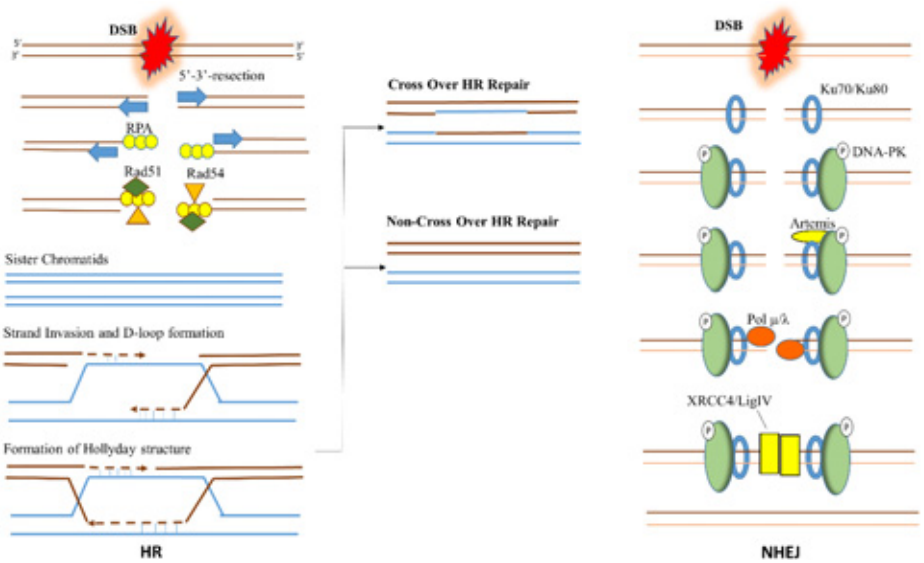

Figure 2: Schematic representation of HR and NHEJ (Modified from (Khalil, Tummala, Zhelev 2012).

Alternative pathways for DSB repair

Beside NHEJ and HR, there are other two alternative pathways that can rejoin a DSB, namely alternative end joining (alt-EJ) and single strand annealing (SSA). Those pathways, which may be initiated after resection, are highly mutagenic and cause oncogenic transformation and genomic rearrangement (Ceccaldi, Rondinelli, D'Andrea 2016). Interestingly, 53BP1 which was considered promotor of NHEJ, is also required for correct progression of HR. In fact, limited availability of 53BP1 triggers the replacement of Rad51 (required for HR) to Rad52 (promotor of alt-EJ) (Ochs et al. 2016). Thus, it seems that 53BP1 is needed for both NHEJ and high fidelity HR.

A closer look at the proteins involved in DNA damage response

53BP1

53BP1 (p53 binding protein 1) is a 220KDa, DNA-binding protein which is a key regulator of the DSB repair processes. Upon DSB induction, 53BP1 becomes hyper-phosphorylated in an ATM dependent manner and it rapidly relocates at the site of the break (Anderson, Henderson, Adachi 2001; Rappold et al. 2001). 53BP1 binds to damaged DNA and forms distinct nuclear foci not only at the site of DSB but also at dysfunctional telomeres, in nuclear bodies and after replicative stress (Harrigan et al. 2011; Lukas et al. ; Rappold et al. 2001; Takai, Smogorzewska, de Lange 2003).

Upon DNA DSB, 53BP1 recognize two histones modifications: H4K20me2 (dimethylation of histone 4 on lysine 20) which is constitutive in the genome and H2A(X) K15Ub (ubiquitinated form of H2AX) which is induced by DNA damage signaling (Botuyan et al. 2006; Fradet-Turcotte et al. 2013). However, H4K20me 2 is usually shielded in the histone core. It is possible that the formation of DSB opens up the chromatin exposing the methylated histone for 53BP1. Recently, the structure of 53BP1 bound to H4K20me2 and to H2AK15ub in a nucleosome core has been revealed at 4.5 Å resolution (Wilson et al. 2016).

The mechanism regulating 53BP1 levels and function are currently unclear. 53BP1 nuclear levels have been reported to drop after exposure to 4 Gy of ionizing radiation. The authors propose that IR induces 53BP1 degradation. However, they suggested that the binding to damaged DNA protects the protein from destruction (Hu et al. 2014). A novel protein, namely Tudor interacting repair regulator (TIRR), has been proposed as key regulator of 53BP1 function. Upon DSB, TIRR dissociate from 53BP1 in an ATM dependent manner, allowing correct DNA binding (Dranè et al., 2017).

The molecular mechanisms behind 53BP1 binding to damaged DNA have been reviewed by (Zimmermann and de Lange 2014). In brief, upon DNA DSB, ATM is recruited at the site of the break and it phosphorylates H2AX to γ-H2AX . Then, MDC1 binds to γ-H2AX and recruits proteins involved in ubiquitination, namely RNF8, UBC13 and UBA1 (Huen et al. 2007). This allows the ubiquitin ligase, RNF168, to bind. RNF168 ubiquitinates H2A or H2AX to H2A(X) K15Ub. 53BP1 recognizes H2A(X) K15Ub and binds to the DNA. Negative regulation of 53BP1 is mediated by de-ubiquitination by

BRCA1, acetylation of histone H4 by TIP60 and degradation of RNF168 (Zimmermann and de Lange 2014).
The role of 53BP1 is to regulate the DSB repair pathway of choice. 53BP1 promotes NHEJ while it inhibits HR. It was shown that 53BP1 is needed for activation of NHEJ in antibody class switch recombination (CSR), in BRCA1 deficient cells, in dysfunctional telomeres and in centromeric heterochromatin (Bothmer et al. 2010; Bouwman et al. 2010; Bunting et al. 2010; Dimitrova et al. 2008; Manis et al. 2004; Noon et al. 2010; Ward et al. 2004). The current view is that 53BP1 prevents HR by blocking resection (Bunting et al. 2010; Zimmermann and de Lange 2014). However, 53BP1 has recently been proposed to play a role in promoting HR fidelity (Ochs et al. 2016).
Initially, 53BP1 has been shown to colocalize with γ-H2AX (Markova, Schultz, Belyaev 2007). However, analysis of the spatial distribution of the proteins in the proximity of a DSB using super resolution STED nanoscopy showed different results. 53BP1 and γ-H2AX occupy different regions of the chromatin (Reindl et al. 2017).
Originally, 53BP1 was identified as a protein that binds to p53 (Iwabuchi et al. 1994). Recently, the mystery around the p53-53BP1 interaction was solved (Durocher and Pelletier 2016). Cuella-Martin et al., (2016) found that 53BP1 promotes the p53-dependent transcriptional response by forming oligomers and by interacting with USP28 protein through its BRCT domain (Cuella-Martin et al. 2016).

53BP1 foci after IR

Ionizing radiation induces formation of 53BP1 foci at the site of DSB. The recruitment of 53BP1 reaches a peak after 20-40 minutes (Hable et al. 2012; Schultz et al. 2000). Studies on the kinetics of 53BP1 showed that the mean time needed for 53BP1 recruitment is similar in different radiation qualities (Hable et al. 2012). However, the appearance of the first foci occurs significantly earlier after heavy ions compared to X-rays. The author propose that more complex damage after high LET radiation induces stronger signal and accelerates 53BP1 recruitment. However, due to big protein size (220 kDa) and possible 53BP1 constitutive binding to undamaged chromatin, the recruitment is slowed down.

DNA-PKcs

DNA-PK catalytic subunit is a protein kinase abundantly expressed in almost all mammalian cells (Hartley et al. 1995). The structure of the protein reveals

the presence of two open channels for binding of double stranded DNA and an enclosed cavity for single stranded DNA (Leuther et al. 1999). DNA-PKcs, together with Ku70/Ku80 forms the synaptic complex that holds the free DNA ends together during NHEJ (DeFazio et al. 2002). Although DNA-PK is mostly studied for its role in NHEJ pathways, this protein interacts with a number of non-NHEJ-related proteins involved in the DNA damage response (Collis et al. 2004). Moreover, it plays a role in telomere capping as shown by the large number of telomere fusions found in DNA-PK deficient cells (Gilley et al. 2001). Thus, DNA-PK is one of the main players in maintenance of genomic integrity as shown by severe combined immune-deficient (SCID) mice with a truncation of the carboxyl terminus of the protein. SCID mice are reported to have premature aging phenotype and non-functional immune system. As expected, DNA-PK deficient cells are radiosensitive and repair DSB incorrectly (Collis et al. 2004).

Tumor suppressor p53

Tumor suppressor p53 is a transcription factor that is involved in a number of cellular responses. When the concentration of p53 increases, it triggers the expression of target genes involved in cell cycle arrest, DNA repair, senescence, and apoptosis; (Symonds et al. 1994; Xue et al. 2007). Moreover, beside these canonical functions, p53 target genes block angiogenesis, induce autophagy, and regulate metabolic processes (Bieging, Mello, Attardi 2014) . p53 protein is known for being a powerful tumor suppressor and it is often called “the master guardian of the genome” (Harris and Hollstein 1993). The gene encoding for p53 protein (TP53) is the most frequently mutated gene in human cancer cells (Petitjean et al. 2007). Indeed, it has been shown that p53 expression stops tumor progression while its mutations increase cellular proliferation and survival (Vogiatzi et al. 2016).

In normal, unstressed cells, p53 is localized in the nucleus where it aggregates, forming monomers, dimers or trimers (Riley et al. 2008). However, upon cellular stresses, several proteins assemble and form active homotetramers (Gaglia et al. 2013). Under normal conditions, p53 is constantly synthetized and degraded with a half-life of 20 min (Weinberg 2007). However, upon a damage signal, posttranslational modifications (mainly phosphorylation) stabilize p53, protecting it from degradation which results in rapid increase of protein levels (Maltzman and Czyzyk 1984). p53 levels are controlled by negative feedback. In fact, p53 induces the expression of the protein responsible for its own degradation, namely MDM2. p53 acts as a transcription factor for the mdm2 gene which codes for the ubiquitin ligase, MDM2 protein (Barak et

al. 1993). MDM2, binds to the p53, and together with MDM4 inhibits its transactivation function (Danovi et al. 2004; Momand et al. 1992; Oliner et al. 1993). Moreover, MDM2 has ubiquitin ligase ability and it ubiquitinylates p53 (Honda, Tanaka, Yasuda 1997). Ubiquitinylated p53 is transported to the cytoplasm where it is degraded by cytoplasmic proteasomes. Phosphorylation is important for p53 activation and stabilization as it prevents the binding of its negative regulators MDM2 and MDM4 (Wade, Wang, Wahl 2010). p53 levels in the nucleus rapidly increase after ionizing radiation (phosphorylation by ATM), after UV radiation (phosphorylation by ATR and ChkII), after hypoxia (unknown pathway), after blockage of transcription and after oncogene signaling or in response to the tumor suppressor protein, ARF (kinases-independent activation) (Bieging, Mello, Attardi 2014) .

ARF binds to MDM2 inhibiting its ubiquitin ligase ability and sequestering it into the nucleoli. MDM2 is therefore unable to mediate the transport of p53 to the cytoplasm for degradation (Zhang and Xiong 1999).

ATM

Ataxia-telangiectasia is an autosomal recessive neurodegenerative disorder characterized by extreme sensitivity to ionizing radiation, neuromotoric dysfunctions due to cerebellar atrophy, impaired immune system, and premature aging among others (Anheim, Tranchant, Koenig 2012; Woods and Taylor 1992). The disease is caused by defects in the ataxia telangiectasia mutated (ATM) gene, which encodes the primary regulator of the DNA damage response: the ATM protein (Savitsky et al. 1995a). ATM is a 350 kDa protein kinase mainly involved in DSB response in every phase of the cell cycle (Pandita et al. 2000; Savitsky et al. 1995b; Shiloh 2001). However, recent studies showed that ATM is activated after other stress responses not necessarily inducing DSB formation. ATM is phosphorylated after hypoxia, hyperthermia, hypotonic- oxidative- and endogenous stress, it is involved in telomere maintenance and dynamics, enzymes synthesis, regulation of the mitotic spindle checkpoint (Paull 2015; Shiloh 2001). In undamaged cells, ATM exists throughout the cell nucleus as homodimers but it dissociates into monomers upon activation (Bakkenist and Kastan 2003). Mechanisms of activation include auto-phosphorylation, phosphorylation by other proteins such as Mre11-Rad50-Nbs1 (MRN) complex or 53BP1, and changes in the chromatin conformation (Bakkenist and Kastan 2003; Lee and Paull 2004; Mochan et al. 2003; Uziel et al. 2003). Upon activation, ATM phosphorylates a number of down-stream proteins involved in both rapid and late DSB response. In the

rapid response, ATM activates checkpoint kinase 2 (ChK2), which in turn phosphorylates cyclin-dependent kinase 25A (CDC25A). CDC25A becomes degraded and induces cell cycle arrest. During the late response ATM phosphorylates p53 which binds to the promotor of p21 leading to apoptosis (in hematopoietic system) or permanent cell cycle arrest (Zgheib et al. 2005).

Mixed radiation fields

Mixed beams of ionizing radiation

Mixed or complex radiation fields are composed of radiation of different quality or energy such as photons and neutrons, gamma rays and electrons, alpha particles and delta electrons (Attix and Tochilin 2016). Complex fields are associated with the majority of environmental, medical and occupational exposure to ionizing radiation. In the environment, mixed radiation is encountered in areas with high levels of radon gas, where the radioactive decay of Ra-226 generates Rn-222 and daughters, emitting alpha particles and gamma rays (Wilson 2000; Wilson et al. 2016). Medical exposures to severe doses of radiation occur mainly during radiotherapy. Cancer patients undergoing radiotherapy receive a curative radiation dose together with an unwanted dose coming from neutrons that are generated in the radiation facility and in the human body (Allen and Chaudhri 1988; Brenner and Hall 2008; Zanini et al. 2004). Moreover, mixed radiation fields are encountered in specific workplaces in nuclear power plants such as high-energy accelerators at CERN where neutrons are accompanied by photons (<10MeV), muons and charged hadrons (>100MeV) (Mayer et al. 2007). Additionally, they are found during civil and military flights at high altitude and in interplanetary space. For pilots and astronauts, the mixed exposure comes from two sources: 1) solar particle events and galactic cosmic radiation which consist of highly ionizing heavy ions and high-energy protons; 2) secondary radiation derived from collision of high energy cosmic rays with air nuclei and aircraft materials (Wilson 2000). While the effect of space radiation on pilots affects merely the ocular lenses, major concern is raising about the cancer risk for astronauts (Cucinotta 2015; Cucinotta et al. 2013; Rafnsson et al. 2005; Sihver et al. 2016). Indeed, radiation exposure is one of the major concern for NASA that is programming a human mission to Mars, where astronauts would be exposed for 3 years to galactic cosmic rays (Cucinotta 2015). The concern about radiation-induced cancer risk is driven by the lack of human data on the early and late effects of

mixed exposure and it is based the assumption of no interaction between the biological effects of the different radiation qualities in the mixed field (Cucinotta 2015; Siranart et al. 2016).

There are several uncertainties associated with the dosimetry and with the prediction of the biological impact of complex radiation fields. For dosimetric purpose, it is necessary to identify the nature and the dose contribution of each component of the field (Horowitz 2006). Several research groups are currently trying to create a complex dosimeter that will be able to estimate the dose contribution and the average ionization density of each field component (Burgkhardt et al. 2006). Promising is the thermoluminescence nanodosimeter that relies on the composite peak 5 in the glow curve of LiF:Mg,Ti for a mixed radiation field that comprises alpha and gamma rays (Sibony et al. 2014). For biological impact, different radiation qualities have different effects, which must be taken into consideration by assigning a specific weighting factor (W_R) to each particle of the field (Joiner and vand der Kogel 2009). However, for mixed fields, the International Commission on Radiological Protection (ICRP) stated:

"*When the radiation field is composed of types and energies with different values of w_R, the absorbed dose must be divided in blocks, each with its own value of w_R and summed to give the total equivalent dose of the mixed field* (International Commission on Radiological Protection 1991).

Thus, given the particle type and the dose contribution of each component of the field, the equivalent dose (H_T) is calculated in Sieverts (Sv) as:

$$H_T = \sum_R W_R \cdot D_{T,R}$$

Where, R is the particle type, W_R is the radiation weighting factor and $D_{T,R}$ is the absorbed dose in a tissue.

In other words, prediction of the effect of exposure to mixed field tries to correlate each particle of the field with the biological endpoint. In the calculation, it is assumed that each radiation quality acts independently so that their effects can be simply pooled together in an additive way (Horowitz 2006). However, this assumption has been proven to be incorrect. A number of experimental studies show that the biological response after exposure to mixed radiation fields is greater than the sum of the individual responses (Mason et al. 2011; McNally, de Ronde, Folkard 1988). Recent studies detected clear synergism at the level of micronuclei and chromosomal aberrations in human peripheral blood lymphocytes, and in the repair kinetics of gamma-H2AX foci in VH10 cells (Staaf et al. 2012b; Staaf et al. 2013). Early investigations showed synergism for in vitro, simultaneous or successive, exposure to neutrons or high

LET particles and X or γ-rays (McNally, de Ronde, Hinchliffe 1984; Ngo, Blakely, Tobias 1981; Railton, Lawson, Porter 1975). Moreover, Brooks and colleagues reported synergistic induction of micronuclei and cell killing after irradiation with constant doses of alpha particles and increasing doses of X-rays (Brooks et al. 1990). However, the evidence for synergism is not strictly clear. Indeed, no significant interaction was observed in the induction of chromosomal aberration in lymphocytes or cell killing in hamster fibroblasts after simultaneous exposure to heavy ions and X-rays (Furusawa, Aoki, Durante 2002). Additionally, experiments on survival of Chinese hamster lung cells failed to detect synergistic effect after exposure to alpha particles (^{238}Pu) and γ-rays (Phoenix et al. 2009). Similar results were achieved after the combined exposure to carbon-beam and X-ray in vitro (Demizu et al. 2004). Even more intriguing are results showing that additive or synergistic effects depends on the time between the first and the second irradiation. While short intervals result in synergistic induction of cell killing, longer intervals (up to 1 day) result in additive effect (Zhou et al. 2006). However, a direct comparison between the above mentioned studies is difficult to make, due to the difference in experimental conditions such as cellular models, end-point considered, sequence of irradiation (simultaneous or successive), radiation qualities, and methods of analysis. More research is therefore needed to clarify when the effect of mixed beams is synergistic and when it is additive.

Possible explanation of synergism

While the initial radiation-induced damage depends on the physical energy deposition, the cellular response is influenced by several factors such as type of lesion, damage recognition, repair pathway of choice, chromatin structure at the site of the lesion, cell type and cell cycle stage (Santivasi and Xia 2014; Venkatesh et al. 2016). As a result, the initial damage is directly proportional to the dose delivered while the response is not always linearly linked to dose (Costes et al. 2006; Neumaier et al. 2012). However, both the initial damage and the cellular response may be affected by the simultaneous action of different radiation qualities. Two radiation types may physically interact and influence the distribution of the ionization events as well as the energy deposition. Therefore, the initial damage could be highly complex and difficult for the cell to repair. It has been suggested that, in the case of combined exposure to high- and low LET radiation, the availability of high-fidelity repair enzymes may be exhausted. Therefore, alternative and error-prone pathways may be activated, resulting in improper repair (Zhou et al. 2006). Another possibility

for synergism is that high LET radiation may exhaust the cellular antioxidant defense mechanisms leaving more low LET-induced ROS free to damage the DNA. Increased oxidative damage may retard the DNA repair processes, induce mutations, and give rise to additional, lethal DSB (Georgakilas et al. 2004; Woods and Taylor 1992; Yang, Galick, Wallace 2004).

Moreover, the protective role of chromatin may fail in a mixed irradiation scenario. Part of the radiation-induced DNA damage (up to 70% for low LET) is mediated by the indirect effect, via products of radiolysis (Hall and Giaccia 2012a). Packed DNA is to some extent constitutively protected from the action of free radicals by the presence of ligands, histones and other DNA binding proteins that shield possible attack sites and/or act as radical scavengers (Isabelle et al. 1995; Warters and Lyons 1992). Damage induced by high LET radiation may disrupt those radical scavengers making the DNA much more vulnerable to the attack of free radicals. Moreover, it has been shown that open chromatin, either constitutive regions of high gene expression (euchromatin) or relaxed chromatin after hypertonic treatment, is more radiosensitive than compact chromatin (Svoboda and Harms-Ringdahl 2005; Takata et al. 2013). Even here, destruction of higher chromatin structure by densely ionizing radiation may open up the chromatin structure increasing the accessibility to damage sites. It must be considered that, usually, high accessibility of DNA areas correlates with better and faster repair processes (Falk, Lukasova, Kozubek 2010). However, this applies to strictly controlled relaxation i.e. through the action of ATM, while disorganization of higher structures after irradiation is linked to deficient repair (Kruhlak et al. 2006b; Kruhlak et al. 2006c; Lavelle and Foray 2014).

Aims

Mixed radiation fields are common in the environment and medicine and pose a challenge for radiation protection. While researchers have reached a consensus about the biological effectiveness caused by high and low LET radiation, the prediction of the biological impact of mixed irradiation is full of uncertainness (Goodhead, Thacker, Cox 1993; Kraft and Scholz 1994). Currently, prediction of the damage is based on the assumption of simple additivity between the effects of all radiations in the field. This assumption has been proven to be incorrect and it underestimates the detrimental effect of combined exposure to different radiation qualities. However, the magnitude of the mixed beam effects is not strictly clear and it requires further investigations. Moreover, the mechanisms behind synergistic effects are still unknown and need to be identified. The aim of this thesis was to investigate the cellular response and the mechanisms behind the effect of mixed irradiation (mixed beams) of X-rays and alpha particles in an attempt to better understand how cells react to simultaneous induction of clustered and dispersed DNA damage (Figure 3).

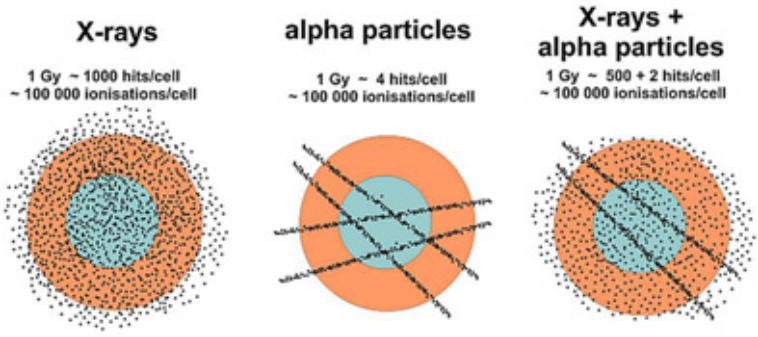

Figure 3. Schematic representation of a cell exposed to different types of radiation. How cells and tissue react to a simultaneous exposure to X-rays and alpha particles is currently unclear.

Specifically, the aims of the thesis were:

- To study whether the effect of mixed beams of X-rays and alpha particles is mediated by oxidative DNA damage. To this end, the cell killing and the mutagenic effect of exposure to different radiation qualities were investigated in lymphoblastoid wild type and BER deficient cells.

- To investigate whether the synergistic effect of mixed beam irradiation is mediated by augmented level of initial damage or by altered cellular DSB repair which leads to delayed DSB rejoining. The initial level of DNA damage and the kinetics of DNA repair was investigated using fluorescent microscopy in fixed U2OS cells or the alkaline comet assay in human peripheral blood lymphocytes. Activation of the DDR was estimated by measuring phosphorylation levels of its key proteins.

- To study whether the live cell dynamics of DSB differs in breaks generated by different radiation qualities. To this end, 53BP1 foci were quantified and qualified in U2OS cells using live-cell microscopy.

Material and Method

U2OS cells

Human osteosarcoma, U2OS, cells were isolated from a sarcoma of the tibia of a 15 year old girl in (Ponten and Saksela 1967). The proteome profile was constructed in 2008 and 237 different gene products were identified (Niforou et al. 2008). This cell line is characterized by chromosomal instability, translocation between chromosomes, and high incidence of aneuploidy (Bayani et al. 2003; Isfort et al. 1995). They have a functional p53 and display p53-dependent cell cycle arrest and activation of checkpoints protein Chk2 (Liu et al. 2009; Lukas et al. 2003). U2OS, with GFP tagged protein 53BP1 were provided by C. Lucas from the Danish Cancer Society, Copenhagen. Characterization of this cell line showing the functionality of the GFP construct was described in (Bekker-Jensen et al. 2005). Cells were cultured in Dulbecco Modified Eagles Medium, supplemented with 10% Bovine Calf Serum and 1% Penicillin streptomycin, in a 5% CO_2 humidified 37ºC incubator.

TK6 cells

TK6 cells are a lymphoblastoid cell line isolated in 1978. They are heterozygous at the thymidine kinase locus and can therefore be used for investigating the mutagenicity of genotoxic agents (Fotouhi et al. 2011; Shakeri Manesh et al. 2014). TK6 are p53-proficient and they are reported to show a non-prolonged G1-arrest following radiation exposure (Little et al. 1995). In contrast to TK6 wild type ($TK6^{WT}$), $TK6^{MYH-}$ cells were stably transfected with shRNA to knockdown hMYH. Western blot analysis confirmed a downregulation of hMYH protein to 5% of the WT´s expression (Shakeri Manesh et al. 2017). hMYH is an important factor of the DNA base excision repair. It removes post-replicative mis-paired Adenine opposite to hydroxylated Guanine (8-oxo-G). Therefore, it prevents somatic G:C→T:A mutations (Jones et al. 2002). Therefore, $TK6^{MYH-}$ cells were expected to accumulate more mutations than WT cells. TK6 and $TK6^{MYH-}$ were grown in suspension in RPMI-1640

medium supplemented with 10% bovine calf serum, 1% PEST and 10mM HEPES in humidified incubator at 37 C^o, 5% CO_2. Cell were kept at density below 2 *10^5 cells/ml during all experiments.

Irradiation

Irradiation was performed in the mixed beam exposure facility, MAX, present at the Center for Radiation Protection Research (CRPR) at the department of Molecular Bioscience the Wenner-Gren Institute, Stockholm University, as described elsewhere (Staaf et al. 2012a). In brief, the facility consists of an alpha source AIF 08 (^{241}Am, total activity 50 ± 7.5 MBq) placed inside an incubator and an YXLON SMART 200 X-ray tube (190kV, 4.0mA) positioned underneath it. For irradiation, coverslips with U2OS cells or cell suspension of TK6 or SY were placed on irradiation dishes. To avoid desiccation, coverslips were covered with 250 µl cell culturing medium. All cells were protected by a thin layer of 1.5µm bilaterally orientated Mylar foil. The irradiation dishes were positioned on a movable shelf between the alpha source and the X-rays tube. Alpha irradiation was started by moving the shelf to the top position, which is close to the alpha source. X-rays exposure was controlled with a semiautomatic switcher. During mixed beam exposure, the X-rays were activated as soon as the movable shelf reached the top position (start of the alpha exposure). This setup allowed for simultaneous exposure to mixed beams of X-rays coming from below the dish and alpha particles coming from above it. Dosimetry of the alpha source was performed by (Staaf et al. 2012a) using track- etched detector and found to have a dose rate of 0.265 Gy min^{-1}. Alpha source had a fluence of 23 789 ± 4564 particles per second and cm^{-1}. The LET of the alpha was calculated based on its fluence and it was found to have average values of 90.92 ± 8.55 keV μm^{-1} with a range that varied between 100 and 170 keV μm^{-1}. In addition, the alpha source emitted beta and gamma radiation with a maximum energy of <70keV and a dose rate of 25 mGy min^{-1}. The dose rate of the X-rays was measured and found to vary between the shelf top position (0.052 Gy min^{-1}) and bottom position (0.068 Gy min^{-1}) (Staaf et al. 2012a). Lead panels shielded the incubator and both AIF 08 and YXLON SMART 200.

Thymidine kinase mutation assay

In vitro mammalian cell gene mutation assay is commonly used to assess the mutagenicity of chemical compounds or ionizing radiation (OECD 1997). In the assay, mammalian cells are exposed to different doses of a test agent. After exposure, cells are incubated several days in normal culture medium to allow phenotypic expression. During this expression time, the DNA damage caused by the test agent becomes fixed in the cells and the wild-type enzyme produced by the target gene is depleted. Mutants are identified due to the acquired phenotypic changes, typically the ability to grow in selective medium (Gad 2008). The gene mutation assay differs procedurally in several ways such as cellular growing conditions and expression time (Kronenberg and Little 1989). However, the main difference between assays is the target gene used for selection. The *TK* gene that codes for the Thymidine kinase (TK) enzyme is often used. The thymidine kinase mutation assay is based on phenotypic changes due to the mutation on the *TK* gene from $TK^{+/-} \rightarrow TK^{-/-}$. Mutants are identified by their ability to grow in TFT-containing medium. In fact, thymidine kinase proficient cells ($TK^{+/-}$) incorporate TFT in the DNA through the *salvage pathway* for TTP production. In contrast, mutants depleted of the functional allele can only use the *de novo* pathway and they are therefore not sensitive to the presence of TFT (Skopek et al. 1978). The mutant frequency can be estimated by calculating the proportion of colonies that form in TFT-containing selective medium (Furth et al. 1981).

The thymidine kinase mutation assay was used in **Paper I** to assess the induction of mutations after exposure to different doses (up to 1 Gy) of X-rays, alpha particles and mixed beams. After irradiation, 1*10^6 cells were incubated in RPMI for 10 days (expression time). To estimate the mutant frequency, 4*10^6 surviving cells were embedded in 0.4% agarose in RPMI supplemented with 5μg/ml TFT. Clonogenic efficiency was estimated from the number of colonies formed in 0.4% agarose in RPMI without TFT. Colonies were counted after 10 days incubation at 37 Co, 5% CO2.

Clonogenic survival assay

The clonogenic survival assay is a widely used biological test to assess the effect of test agents on cell proliferation. Exposure to toxic agents can have several effect on mammalian cells. Depending on the dose, cells may continue to proliferate, become senescent or go into apoptosis/necrosis. The clonogenic assay estimates the percentage of cells that retain the mitotic integrity after exposure to toxic test agent, i.e. ionizing radiation. In this is assay, exact numbers of irradiated cells are seeded out into culture vessels and allowed to grow until colonies with at least 50 cells are formed. The plating efficiency (PE) is calculated as the percentage of seeded cells that grow into colonies while the surviving fraction (SF) is given as:

$$SF = \frac{number\ of\ colonies\ counted}{number\ of\ cells\ seeded * PE}$$

Cell survival curves are then constructed by plotting the surviving fraction on a logarithmic scale against dose on a linear scale (Hall and Giaccia 2012b).The clonogenic survival assay was used in **Paper I** to estimate the surviving fraction of TK6 cells. After irradiation, cells were collected, counted and casted in 0.4% agarose:RPMI, 1:1, followed by 20 min incubation at 4 C^{o} to allow the agarose to solidify. Colonies were counted after 14 days at 37 C^{o}, 5% CO_2.

Alkaline comet assay

The single-cell gel electrophoresis or comet assay is a widely used technique to asses DNA damage in individual cells. In this assay, cells are embedded in an agarose gel on objects slides and lysed. Lysing releases the DNA, which is forced to migrate through the gel by constant electric field. If DNA is fragmented due to strand breaks, it will migrate forming a structure that reminds of a comet. The head of the comet represents the portion of intact DNA, while the tail contains the damaged DNA. Since the frequency of DNA breaks is linear with the proportion of DNA in the tail, the comet assay detects and quantifies DNA damage (Collins 2004). The comet assay is a versatile and straight forward technique, and it is therefore used in genotoxic testing, ecotoxicology, human biomonitoring, molecular epidemiology and fundamental research in DNA damage and repair (Burlinson et al. 2007).
Depending on the DNA damage of interest, different variants of the assay can be applied. The assay performed under alkaline conditions, the alkaline comet

assay, relies on a high pH to unwind the DNA from double to single stranded. A break on any of the two strands will give rise to DNA fragments able to migrate through the gel. The alkaline comet assay can therefore detect both single and double strand breaks in addition to apurinic sites which are converted to breaks by the alkali conditions (Burlinson et al. 2007).
The alkaline comet assay was used in **Paper IV** to estimate the initial level of DNA damage and the kinetics of DSB repair after radiation exposure to different radiation qualities. The assay was performed with whole blood as described by (Wojewódzka et al. 1998) with slight modifications.

Western blotting

Western blotting, or immunoblotting, is a widely used biochemical technique to detect particular proteins of interest in a complex mixture of tissue homogenate or cellular extract. In Western blotting, proteins are separated through polyacrylamide gel-electrophoresis. In practice, proteins are loaded on a SDS-polyacrylamide gel and immersed in a SDS buffer that makes them negatively charged. Upon application of an electric field, proteins migrate towards the positive pole. Based on their molecular weight, proteins migrate at different speed though the gel and therefore they separate. Proteins are later transferred onto a porous membrane and stained with specific antibodies for detection (Lodish et al. 2000). Western blot was used in **Paper II** to investigate changes in levels of protein phosphorylation following radiation exposure. Proteins of interest were: DNA-dependent protein kinase catalytic subunit (p-DNA-Pkcs); Ataxia Telangiectasia Mutated (p-ATM); tumor protein 53 (p-p53); Glyceraldehyde-3-phosphate dehydrogenase (GAPDH).
p-DNA-PKcs, with a molecular weight of 470 kDa, has a key role in NHEJ pathway; p-ATM, which has a molecular weight of 350 kDa, is a master controller DNA damage signaling pathway. p-p53, which has weight of 53 kDa, was chosen because it is the main guardian of the genome. Finally, GAPDH (37 kDa) which is a key enzyme of glycolysis, was used as housekeeping gene since its expression is not altered by radiation exposure (Banda et al. 2008).

Fixed cells vs live-cell analysis

Cellular processes may be investigated by imaging snapshots of fixed cells or by directly recording time-lapses of live cells. The live-cell technique offers the clear advantage of insight into the dynamics of cellular processes such as organ development, chromatin movements, and protein recruitment. However, there are a number of issues related to live-cell experiments. First, cells need to survive the live-cell experiments. This implicates that environmental conditions such as temperature, air humidity, nutrient and oxygen concentration must be strictly controlled in experiments lasting more than a few hours. Other problems are phototoxicity and photobleaching. Illumination, especially if imaging requires high intensity light may damage the cells and halter their behavior as well as it may bleach the fluorescent probes. Therefore, researchers rely on taking pictures at less frequent intervals and with low illumination (often resulting in poor image quality) in order to minimize photo bleaching and toxicity. Moreover, migrating cells and focus drift represent a big challenge during long time imaging. Healthy cells constantly crawl and they may migrate out of the imaging plane. In addition, following single cells in dense and highly mobile culture is not an easy task and it requires short intervals imaging. Focus drift may depend on different factors such as intrinsic cellular movements, vibration of the microscope and temperature changes. Finally, storage and analysis of large data sets may overload standard lab computers (Baker 2010). In **Paper III**, cells were imaged after radiation exposure in a temperature-controlled live-cell chamber mounted on a Carl Zeiss Axiovert 200 inverted microscope at 37 ^{o}C and normal oxygen concentration (Scherthan and Adelfalk 2011). Shift of the pH in the cellular medium due to oxygen exposure was prevented by adding sodium pyruvate and 10 mM HEPES (Ettinger and Wittmann 2014). Imaging exposure-time was limited to 200 msec. Due to the sub-optimal condition of the live-cell chamber, imaging was restricted to 75 min. During that time cellular shape, volume and movements were carefully monitored to detect any change in cellular behavior due to the imaging conditions. However, the major challenge in the live-cell experiments was represented by focus drift, which made the majority of experiments impossible to analyze.

Gathering of 53BP1 protein in distinct nuclear foci was investigated in fixed cells in **Paper II** and with live-cell microscopy in **Paper III**. Besides the imaging acquistion (snapshot of fixed cells vs time laps of individual cells), the major difference between the two papers was the image analysis. In **Paper II,** the time of image acquisition was increased until all foci in the focal plane

could be detected. This resulted in a higher focus frequency detected in fixed cell experiments as compared to live ones. Since focus intensity was set to maximum, this parameter was not taken into consideration in **Paper II**, while it could be quantified in **Paper III**. Image analysis of pictures of fixed cells was performed with ImageJ while the upgraded version of it, Fiji, was used in the live-cell experiment (Schindelin et al. 2012; Schneider, Rasband, Eliceiri 2012).

The image analysis of the life cell pictures required two steps of picture manipulations:

- Rigid body transformation, used to immobilize the highly mobile nuclei.
-Smoothing, used to have clearer focus edges.

In this analysis, focus intensity was not increased and foci were detected according to thresholding. In practice, a threshold was chosen for focus intensity that would apply to all pictures in a time lapse series (corresponding to a movie). Small, low intensity foci often remained undetected. Indeed, a comparative measurement of areas of the smallest foci detected in fixed cells and live-cells revealed that the smallest focus area detected in fixed cells was 0.1 μm^2 while it was 0.25 μm^2 in live cells. This difference was not likely to influence the large, alpha-induced foci, but it probably influenced the detection of small X-ray and mixed beam-generated foci.

In addition to image analysis, the shape of nuclei differed in the two imaging techniques. Fixation in paraformaldehyde made the nuclei of fixed cells flat. Therefore, more foci were detected in the focal plane of fixed cells compared to live ones. This factor is likely to have influenced the total number of foci generated by the X-rays, which form sparsely in the nucleus. In contrast, it was unlikely to have had an impact on the foci generated by alpha particles that traverse a big part, if not all, of the nucleus.

R software

R software was used for carrying out the majority of the analysis in **Paper III.** "R" is a high-level programming language and an environment for statistical computing. It was designed by Robert Clifford Gentleman and Ross Ihaka (R&R) in 1993 at the University of Auckland, New Zeeland. Today, "R" is an open-source project, driven by the core team, which is responsible for the software source, and by the internet community, which provides packages to extend R capabilities (Crawley 2012). The packages implement diverse R-functions, from specialized statistical techniques (i.e. package survival) to high quality, interactive graphical visualization (i.e. package ggplot2 and plotly). There are more than ten thousand packages and their number is constantly increasing. All the packages are well documented, uniformly structured, and they are stored in open source repositories such as CRAN, R-Force and Bioconductor (Hornik 2012). Moreover, the R community offers tutorials and internet support to all R users that get stuck with any kind of R-related problems (R Core Team 2016). In summary, the high-level graphical visualization together with the versatility of the language and the constant support, largely compensate for the steep learning curve of the quite complicated R language. The following figures are example of R graphical visualization. Figure b) and c) were generated by simply writing the following codes:

library (plotly)
nucleus <- readTIFF ("alpha 70 min.tif")
plot_ly (z = as.matrix (nucleus) , type = "surface")

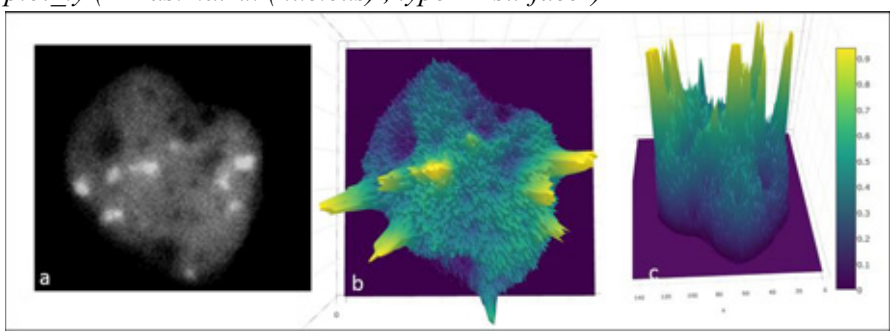

Figure 4: Example of data visualization with R. Nucleus of U2OS cancer cell 70 min after alpha irradiation. a) Original picture; b) 3D surface plot of the same cell nucleus created with the package "plotly"; c) Interactive 3D surface plot showing the peaks of intensity.

Mean Squared Displacement

Movements of objects or particles may be quantified using a mean-squared displacement (MSD) analysis (Berg 1993). In this analysis, the exact position of a particle or a locus is recorded in multiple time-lapse series and the average of its squared distance is plotted against time. MSD is calculated as $<(x_t - x_{t+\Delta t})^2>$ where t is the time and x is the exact position of the moving particle (Berg 1993). The shape of the MSD curve is indicative of the type of movement. Linear relationships, where the values of MSD increase constantly with time, are characteristic of pure random walk (Brownian motion). In this case, particles are free to move in space and the only restriction is represented by collision with other particles. However, if movements are constrained by a physical barrier, i.e. the nuclear membrane, the MSD curve will reach a plateau. In contrast, an exponential curve is created by particles displaying directed motion. Beside the shape of MSD curve, the most used quantitative parameters are the diffusion coefficient and radius of constrain (Rc). In pure Brownian walk, the diffusion coefficient is directly proportional to the temperature of the medium and it equals the slope of the linear curve (Berg 1993). In contrast, the radius of constraint is not temperature dependent and it is calculated from the plateau in a constrained movement curve (Weber, Spakowitz, Theriot 2010a; Weber, Spakowitz, Theriot 2010b). MSD analysis were used in **Paper III** to compare the movements of DNA DSB that were induced by different radiation qualities.

Figure 5 The shape of the MSD curve is indicative of the type of movement

Results and Discussion

Paper I

In previous studies, we detected synergistic effects between the action of X-rays and alpha particles in the induction of micronuclei and in the yield of complex aberrations in peripheral blood lymphocytes (Staaf et al. 2012b; Staaf et al. 2013). It can be supposed that this effect can occur by different mechanisms. The simultaneous exposure may lead to increased LET and damage complexity, it may overwhelm cellular defense mechanisms or it could lead to higher levels of oxidative damage. In **Paper I** we were interested in testing whether the interaction of alpha radiation and X-rays leads to increased action of low LET-induced oxidative damage. We expected that this effect would become clearly visible when the level of alpha-induced damage was kept at a constant level, while the level of X-ray damage was changed. Therefore, the dose of alpha particles was set at 0.2 Gy, which correspond to an average of one hit per cell nucleus, while X-rays dose was constantly increased. Moreover, if oxidative damage to DNA is increased during mixed irradiation, this effect should be strongly expressed in cells that are sensitive to ROS. Therefore, clonogenic cell survival and induction of mutations were investigated after radiation exposure in two lymphoblastoid cells lines, namely $TK6^{WT}$ wild type, and $TK6^{MYH-}$. While $TK6^{WT}$ cells were BER proficient, $TK6^{MYH-}$ cells expressed low levels of the glycosylase hMYH and therefore had a reduced ability to remove oxidative damage from the DNA (Shakeri Manesh et al. 2017). hMYH is a BER repair protein that acts after replication by removing adenine when mis-paired with the guanine adduct (8-oxo-dG). The SSB that results from the removal of adenine is repaired by high fidelity DNA polymerase lambda that inserts cytosine restoring the original sequence (Friedberg et al. 2006) Thus, functional hMYH prevents G:C to T:A transversion mutations, while lack of this protein results in an increased yield of mutations (Mazzei, Viel, Bignami 2013; Ruggieri et al. 2013). However, the SSB produced during the repair process may cause complications for the cells. Overactivity of hMYH may induce futile base excision repair cycles in which an adenine is repeatedly reinserted opposite an 8-oxoG by low fidelity DNA polymerases

such as pol β and pol κ. The futile BER cycle would cause persistent accumulation of hMYH-generated breaks, inducing p53-mediated apoptosis (Hashimoto et al. 2004).

As expected, the survival curves of both cell lines followed a linear relationship after alpha particles and mixed beam while they were best described by the linear quadratic model for X-rays. Analysis of the envelope of additivity on the clonogenic survival of $TK6^{WT}$ and $TK6^{MYH-}$ showed that mixed beam of X-rays and alpha particles had synergistic effect on the survival of $TK6^{WT}$ but not $TK6^{MYH-}$. Interestingly, $TK6^{MYH-}$ were found to be more radioresistant than wild type cells. The results can be explained with focus on the post-replicative role of hMYH. Under the condition of oxidative stress, 8-oxoG may accumulate in template DNA leading to overactivity of hMYH and induction of p53-mediated apoptosis. Thus TK6 cells, which are prone to go into p53-mediated apoptosis, survive better after radiation exposure in absence of hMYH. Although the mechanisms for the observed synergistic effect were not elucidated, the outcome of clonogenic survival suggests that oxidative DNA damage plays an important role in the lethal effect of mixed beam. We hypothesize that in the case of mixed beam, disruption of higher order chromatin structures by alpha particles may open up the DNA and render it more vulnerable to the attack of free radicals. Moreover, hits from alpha particles may exhaust the cellular antioxidant defense leading to increased level of X-rays-induced oxidative damage.

Since $TK6^{MYH-}$ were not able to sense or repair A:G lesions in the DNA, this cell line was expected to accumulate more mutations than wild-type cells, with this effect being more pronounced under oxidative stress. We quantified mutations by estimating the mutant frequency after radiation exposure. Mutants carrying the homozygous $TK^{-/-}$ gene, were identified by their ability to proliferate in TFT-containing selective medium. As expected, we found that the rate of spontaneous mutations was 6-folder higher in $TK6^{MYH-}$ than in wild type cells. However, in both cell lines, no synergistic effect could be detected at the level of mutant frequency after exposure to mixed beam of alpha particles and X-rays. The lack of correlation between the results of the clonogenic survival and the cellular response at the level of mutations may be due to the interexperimental heterogeneity of the results. Induction of mutation in one specific locus among all the genome is a rare, stochastic event and it is difficult to spot. Moreover, the identification of mutants is influenced by the balance between survival and mutation induction. High radiation doses that should increase the probability of detecting mutations may, in fact, have an overkilling effect (Hall and Giaccia 2012a). Thus, at higher doses, heavily mutated cells may

simply not survive. The overkilling effect was probably more pronounced in $TK6^{MYH-}$ cells that displayed a much higher level of baseline mutations than in wild type cells.

Major finding in **Paper I:**

- Synergistic effect of alpha particles and X-rays in inducing cell killing in TK6 wild type cells.
- Additive effect of mixed beam in survival of cells with reduced ability to repair oxidative damage.
- Oxidative DNA damage plays an important role in the lethal effect of mixed beam.

Paper II

In **Paper II**, we investigated whether mixed beam exposure leads to an augmented DSB induction or an altered response of the cellular DDR machinery. Bone cancer cells, U2OS, stably expressing 53BP1-GFP fusion protein were used as the cellular model. 53BP1 is a DSB sensor protein that gathers at the site of DSB, forming nuclear foci. The induction and the disappearance of foci after exposure to alpha particles, to X-rays or to a mixed beam of both were considered as evidence of DSB formation and repair. The mixed beam consisted of 50% alpha particles and 50% X-rays. Two types of analysis were performed: 1) dose response relationship of 53BP1 focus induction, where focus frequencies were measured 30min after exposure; 2) kinetics of focus decay, where frequencies of foci were quantified at defined intervals after exposure to a dose of 1Gy. Moreover, the levels of phosphorylated ATM and p53 proteins were quantified as markers of activation of the DNA DSB response.
Analysis of the distributions of focus areas after different radiation doses showed that all tested radiation qualities induced two types of foci. Small Foci (SF), which displayed an area smaller than 0.5 μm^2, and Large Foci (LF) with an area bigger than 0.5 μm^2. The size of foci has been proposed to reflect the level of damage clusters (Aten et al. 2004; Costes et al. 2006; Jakob, Splinter, Taucher-Scholz 2009; Jakob et al. 2005) with larger foci indicating complex lesions. Hence, we expected to detect a difference in focus induction and repair depending not only on radiation quality but also on focus type. Indeed, we found that alpha radiation, which is known to induce complex damage, produced a higher yield than X-rays and mixed beam, for doses up to 1Gy. At higher doses, the focus frequencies became saturated for all radiation qualities probably due to focus confluency. Hence our results strongly indicate that LF can be considered as synonymous for complex damage, while SF probably represent simple breaks.
The hypothesis of a synergistic effect between the action of alpha radiation and X-rays in generating DNA damage was tested by constructing the envelopes of additivity. The envelopes showed that alpha particles and X-rays interact and induce DNA damage in a synergistic way for all tested focus levels. Moreover, analysis of the 53BP1 focus repair kinetics showed that the decay in focus frequency was strongly influenced by radiation quality. While all foci displayed a sharp decline few hours after exposure, this decline was lowest after mixed beam. Thus, our results show that mixed radiation induce DNA DSB in a synergistic way. Moreover, mixed irradiation-produced foci are con-

sistently removed more slowly than expected based on simple additivity between X-rays and alpha particles. This effect was visible at the level of SF and it was particularly evident in the initial decay of LF.

One of the hypotheses behind the synergistic effect of the mixed beam is the increase in energy deposition, LET, and consequently of DNA damage complexity. Complex damage induces the formation of large DNA-repair foci (Aten et al. 2004; Jakob, Splinter, Taucher-Scholz 2009; Rall et al. 2015). Thus, increased damage complexity as a result of mixed irradiation, should be detectable at the level of 53BP1 focus size. However, we could not detect any increase in values of focus area due to mixed irradiation. Therefore, our results do not support the hypothesis of increased LET due to interaction between different radiation qualities.

Another possibility to the synergistic effect could be that the damage induced by high LET radiation may exhaust the DNA repair mechanisms (Greubel et al. 2008). Therefore, alternative and error-prone pathways may be activated to deal with the remaining DNA damage, resulting in delayed or improper repair. If mixed irradiation of X-rays and alpha particles overwhelms the DSB repair machinery, one would expect to detect slow elimination of 53BP1 foci. Indeed, our results showed that the initial decay of mixed beam-induced foci proceed at a slower rate than expected based on the assumption of simple additivity between alpha and X-rays. This effect was mainly due to slower initial decay of LF (synonymous for complex damage). Thus, our results indicate that the DSB repair system is indeed overwhelmed by the simultaneous exposure to X-rays and alpha particle, which results in the delay of damage processing.

Interestingly, the half-life of radiation-induced foci was strongly dependent on radiation quality. For alpha and mixed beam, the SF were repaired at faster rate than the respective LF, probably reflecting the complexity of the damage. In contrast, both SF and LF produced by X-rays had the same half-life of 2h. All foci formed after mixed irradiation were eliminated with a slower kinetics than those produced by X-rays but with a faster kinetics than those induced by alpha particles.

The proportion of LF and SF among all foci was dependent on radiation quality but it was not influenced by the dose. Not surprisingly, alpha particles induced mainly LF. In contrast, X-rays generated similar proportion of LF and SF. Keeping in mind that the mixed beam is composed of 50% alpha and 50% X-rays, one would expect that the foci produced by this irradiation should have a large proportion of LF (due to the LF induced by alpha particles). However, this was not detected. Mixed beam produced similar proportion of LF

and SF. Hence, the synergistic effect that was observed at the level of initial foci must be mediated by higher induction of simple damage. Those results further confirm that the simultaneous effect of alpha particles and X-rays does not lead to increased LET and damage complexity. Rather, the synergistic effect seems to be mediated by increased yield of simple DSB.
In summary, results of **Paper II** demonstrate that simultaneous exposure to alpha irradiation and X-rays results in a synergistic induction of DNA damage. Although more research is needed to fully elucidate the mechanisms behind the detected synergistic effect, our results strongly suggest that overwhelmed DNA-repair system causes delay in repair of both simple and complex damage.

Major finding **Paper II**

- Alpha particles and X-rays interact and induce DNA DSB in a synergistic way for all the focus frequencies that were tested.
- Mixed beam irradiation alters the cellular repair dynamics compared to cells exposed to a single radiation type.
- The decay of mixed beam-induced 53BP1 foci proceeds at a slower rate than expected based on simple additivity between the action of alpha particles and X-rays.
- This effect was mainly due to a reduced initial decay of foci that were larger than 0.5 μm^2.

Paper III

Since the synergistic effects on the repair of 53BP1 foci was particularly pronounced in the initial decay of foci, we decided to further investigate the initial events post irradiation. In **Paper III**, we employed 2D time-lapse microscopy and semiautomatic image-analysis to investigate the dynamic behavior of radiation-induced 53BP1-GFP foci in U2OS cells during the first 75 min after radiation exposure.

Quantification of the frequencies of foci per cell (FPC) showed that all three radiation qualities induced a strong increase in the frequency of FPC shortly after irradiation. Foci frequencies reached a maximum at 16 min p.r. after X-rays, at 11 min after alpha particles and at 9 min after mixed irradiation. Non-irradiated cells had on average 1.5 FPC during the imaging time. Spontaneous foci were likely to represent sites of unrepaired DNA damage. As expected, the sparsely ionizing X-rays induced the highest frequency of FPC while the densely ionizing alpha particles generated the lowest frequencies. Surprisingly, in contrast to the results achieved in Paper II, the frequencies of FPC after mixed irradiation showed intermediate values between the effect of alpha particles and X-rays. However, due to different image-acquisition, manipulation, and analysis, the results of focus frequencies in the Paper II and the present investigation are not directly comparable. Indeed, in the present analysis small, low-intensity foci fell below the detection level. This difference is not likely to influence the number of foci detected after alpha particles, which induces mainly large foci with high intensity. However, it had a strong impact on the detection of foci in nuclei exposed to X-rays and mixed beam.

The kinetics of focus disappearance was radiation-specific. X-rays displayed the strongest decrease in focus frequency followed by alpha particles and mixed beam. Interestingly, mixed beam irradiation, which consisted of 0.5 Gy X-rays and 0.5 Gy alpha particles, showed a kinetics of focus loss slightly slower than after 1 Gy alpha irradiation alone. Based on the assumption of simple additivity, one would expect that, the part of X-ray-induced foci would disappear (at least) as fast as those produced by X-rays alone. Thus, at least, 43% of the X-ray-induced foci should have been repaired within the imaging time. The same logic could be applied to the alpha-induced foci. Even here, one would expect that 15% of the alpha-induced foci would disappear within the imaging time. However, this was not the case and only 10% of all the mixed beam-induced foci did disappear at the end of imaging time. Thus, the kinetics of foci appearance and decline after mixed irradiation cannot be described as a simple average response to X-rays and alpha particles. Our results

show that, mixed beam-induced foci showed a kinetics of focus disappearance similar to that of pure alpha irradiation.

We next asked whether the difference in the kinetics of focus appearance and decline after mixed beam irradiation was related to changes in focus size. 53BP1 binds at the site of DSB to signal the damage to DNA repair proteins. As several DSB form in close proximity, more 53BP1 molecules bind to DNA. It has been calculated that high LET irradiation induces clustered DSB and complex DNA damage (Nikjoo et al. 1998), therefore, we assumed that the area of 53BP1 foci could be positively correlated with clustered DSB. In agreement, our results showed that alpha radiation produced foci with the largest area compared to X-rays and mixed beam. However, the latter two radiation qualities produced foci of similar size. Thus, the lack of fast decrease of focus frequency after mixed beam irradiation was not related to large focus size.

Our live-cell imaging system allowed capturing of 2-D images. Quantification of the focus area was, therefore, limited to the XY plane. To have a better characterization of 53BP1 foci, we quantified the average focus intensity, which is another parameter that directly correlates with the amount of 53BP1 molecules present in a focus. Our results showed that foci induced by mixed beam reached the highest intensity during the first 40 min after exposure. This result indicates a strong concentration of 53BP1 molecule in mixed beam-induced foci, probably in those induced by the traversal of an alpha particle. Consequently, small and disperse foci produced by X-rays may have fallen below the detection level.

Quantification of focus mobility (displacement) was performed with ImageJ software and mean squared displacement (MSD) analysis. The shape of the MSD curve showed that the movements of 53BP1 foci could be described as random walk (Brownian) in a confined space with subdiffusion parameters. Moreover, we detected that the mobility of 53BP1 is radiation-specific. Alpha-induced foci displayed the highest degree of focus movement, followed by those induced by X-rays and mixed beam. The role of movements of damaged DNA is currently a matter of discussion (Dion and Gasser 2013; Lottersberger et al. 2015). It has been proposed that mobility, which require intact microtubule and the LINC complex, may be an ”error correction mechanism”, where higher mobility increases the probability of correct repair (Lottersberger et al. 2015). However, chromatin mobility is constricted by crowding-induced viscoelasticity (Weiss et al. 2004). Our results detected lower displacement in mixed beam-induced foci. We suggest that restricted mobility is linked to the observed delay in focus clearance. Moreover, mixed beams mobility may have

been influenced by the presence of undetected simple DNA damage, or damaged cellular structure such as the microtubules.
We next asked whether the mobility of DSB-containing chromatin regions resulted in interactions between foci. We observed that roughly 30% of the radiation-induced 53BP1 foci within a nucleus showed interacting behaviors. Foci merged, split and sometimes they merged only to split again few minutes later. Quantification of the merging behavior showed that ionizing radiation predominantly induced focus merging. Alpha particle irradiation showed slightly higher percent of merging foci than X-rays and mixed beam. This trend correlated well with the results from the MSD, where alpha particles were the radiation type with the largest displacement. However, the observed large internuclei variability suggests that the merging is more likely a cell cycle-related event rather than a general.

Major findings **Paper III**

- The effect of mixed beam in inducing DSB signaling foci can seldom be described assuming additivity between the effect of alpha particles and X-rays.
- Regarding foci induced by mixed beam:
    - They show a kinetics of focus disappearance similar to that of pure alpha irradiation.
    - They display more restrict movements than those produced by alpha particles and X-rays.
    - Their size is similar to X-rays induced foci.
    - They have the brightest intensity suggesting a strong attraction of 53BP1 molecules.

Paper IV

In Paper II and III, radiation-induced DSB were investigated in cancer cells. In contrast, the experiments performed in **Paper IV** focused on the radiation-response in normal cells. We used the alkaline comet assay, which can detect not only DSB but also AP sites and SSB, to quantify the level of DNA damage and the kinetics of damage repair after radiation exposure in human peripheral blood lymphocytes. The comet assay has its name from the comet-like tail formed by fragments of broken DNA. The percentage of DNA contained in the comet tail (relative tail intensity, RTI) was used as measure of the level of DNA damage after exposure to alpha particles, X-rays or mixed beam (1:1 alpha: X-rays). Activation of DNA damage response was detected by measuring phosphorylation levels of DNA-PKcs, ATM and p53 by Western blot.

Dose-response relationship of the RTI after alpha particles was significantly lower than after X-rays and mixed beam. The latter two radiation qualities displayed similar levels of DNA damage. Since alpha particles, which induces predominantly complex damage showed the weakest dose response, and all radiation qualities induced saturation of values of tail intensity at higher doses, our results strongly indicate that the detected relative tail intensity is inversely proportional to damage complexity.

Results of the envelopes of additivity showed that the initial level of damage after mixed beam is higher than expected assuming simple additive effects between alpha particles and X-rays. Interestingly, the strongest interactions were detected at low levels of damage.

The kinetics of DNA repair detected with the comet assay was not dependent on radiation quality. In contrast, the distributions of RTI at various time points after irradiations were different in cells exposed to alpha particles, X-rays or mixed beam. Distributions of RTI after alpha particles stayed relatively stable until 180 min *p.r.* where ongoing DNA repair became clearly detectable. In contrast, the frequency of cells with high RTI decreased already at 15 min post X-rays irradiation, indicating rejoining of DNA fragments. Interestingly, the distribution of RTI immediately after mixed beam exposure was similar to those of X-rays. However, the frequency of cells with high RTI decreased at slower rate than after pure X-rays irradiation. Thus, our results suggest that the initial level of damage after mixed beam is similar to that of X-rays, however, the repair of it occurs with delay.

In summary, the results indicate that alpha particles and X-rays interact and generate more damage than expected based on the assumption of simple additivity between the two radiation qualities. Moreover, the DNA repair machinery is impaired in mixed beam irradiation.

Major findings **Paper IV**:

- Synergistic effect between the action of alpha particles and mixed beam at the level of initial DNA damage.
- Repair of DNA damage in cells exposed to mixed beam occurs with delay.
- Phosphorylation levels of ATM and p53 are significantly higher after mixed beam at 1h and 3 h post irradiation.

Conclusions and future studies

Mixed radiation fields are associated with a simultaneous action of different radiation qualities. Currently, calculation of the biological effect of mixed radiation fields does not take into consideration the possibility of an interaction between different radiation qualities. The results presented in this thesis indicate that the default assumption of simple additivity between the effects of all the particles in a mixed radiation bream is incorrect and should be reviewed. Our results clearly indicate that simultaneous exposure to alpha particles and X-rays generates biological damage synergistically. Moreover, the damage produced by mixed irradiation overwhelms the DNA repair machinery leading to slow repair.

The results are important from the perspective of radiation protection. They suggest that the cancer risk factors extrapolated from the Life Span Study (Hiroshima and Nagasaki survivors), who were exposed to a mixed fields of neutrons and gamma rays, may be overestimated when applied to predict effects of pure low of pure high LET radiation exposure. At the same time, calculations of secondary cancers as a results of radiotherapy could be underestimated if they are carried out based on assuming additivity of low and high LET radiations. Although the scale of the synergistic effect at the level of cancer induction cannot be derived from the results, the data demonstrate a source of uncertainty when health risk factors are transferred between groups of people exposed to different radiations. Also, the results are interesting from the perspective of how cells cope with clustered and dispersed DNA damage induced simultaneously. In view of the above, the magnitude and the mechanisms behind the synergistic effect in simultaneous exposure should be further investigated. The results in **Paper I** suggest that the indirect effect of radiation plays an important role in the synergistic effect of a mixed beam of alpha particles and X-rays. The involvement of oxidative damage could be further verified by using radical scavengers such as DMSO or agents that induce oxidative DNA damage such as bromate (Bajinskis et al. 2013; Zhang et al. 2010). Moreover, it would be very useful to compare the results of **Paper II** with Monte Carlo simulations generated with the PARTRAC code which could calculate the theoretical radiation hits as well as the biological damage.

One of the observation made during live-cell imaging in **Paper III** is that the damaged chromatin is highly dynamic, with 53BP1 foci appearing and disappearing constantly. A non-quantified number of foci did in fact appear long after the reported time for maximum foci induction (more than 30min). Due to limitation in the imaging technique used in this study, it was not possible to determine if those late-appearing foci emerged from lower parts of the nucleus due to movements of the chromatin, which brought the already existing foci up in the focal plane, or if those foci were indeed formed with delay. Understanding the mechanisms behind double strand breaks movements and the late-appearing foci could give important insights on DSB recognition and repair.

Moreover, some nuclei displayed nearly immobile foci while other nuclei had highly interactive foci. It would be interesting to further investigate whether damage chromatin behave differently in different phases of the cell cycle in mammalian cells. To this end, cell synchronized simply by mitotic shake-off and exposed at different cell cycle stages.

Appendix

Conference and workshop presentations (2012-2016)

- **Sollazzo, A**., Shakeri-Manesh, S., Fotouhi, A., Czub, J., Haghdoost, S. & Wojcik, A. Swe-rays mutant frequency and clonogenic survival of human lymphoblastoid cells exposed to mixed beams of alpha particles and X-rays. Swe-rays workshop, August 2013. Uppsala. *TALK*

- **Sollazzo, A**., Brzozowska, B., Cheng, L., Lundholm, L., Haghdoost, S., Scherthan, H. & Wojcik, A. Alpha particles and X-rays interact in inducing DNA damage in U2OS cells. Swe-rays workshop, August 2016. Stockholm University. *TALK + Shooting Star-award for best presentation*

- **Sollazzo, A**., Brzozowska, B., Cheng, L., Lundholm, L., Haghdoost, S., Scherthan, H. & Wojcik, A. Alpha particles and X-rays interact in inducing DNA damage in U2OS cells. Nationellt möte om sjukhusfysik. November 2016. Kolmården, Sweden. *INVITED TALK*

- **Sollazzo, A**., Brzozowska, B., Cheng, L., Lundholm, L., Scherthan, H. & Wojcik, A. Live dynamics of 53BP1 DNA damage foci induced by different radiation qualities. National DNA metabolism meeting. January 2017. Stockholm University. *INVITED TALK*.

Acknowledgments

When I started my PhD studies, I naively believed that it would be like sailing on smooth sea. Soon reality caught up and I realized that this journey would have never been possible without the help and support of many others.

Firstly I would like to express my deepest gratitude to my supervisor Andrzej Wojcik who gave me the opportunity to start as a PhD student. Thanks Andrzej for being a great supervisor, for all the support, for the scientific discussions as well as for repairing malfunctioning microscopes, leaking cell chambers and the help in writing manuscripts. Thanks also for organizing skiing trips and interesting study visits to nuclear power plants or mines in search for any sign of radioactivity.

I would also like to thank my co-supervisor Siamak Haghdoost. Thanks for all the lab techniques that you have taught me as well as for gathering people for "fika-time". Thanks to Mats Harms-Ringdahl for the precious discussions about my licentiate thesis, and thanks for making the working environment such a pleasant place to be. It is great to see pictures of you sailing or flying around in Stockholms skärgård!

I would also like to thank prof. Harry Scherthan for the valuable and continuous support during the last year of my PhD studies. I could always count on your support for any microscope-related issue, image analysis as well as interpreting data and getting new ideas! Thanks a lot for all that!

A big thanks goes to all in the radiobiology group:

To Lovisa Lundholm, thanks for your professionality and for always being there when needed! Thanks for correcting all the "s" in the wrong places in my writings and for cheering me up when "*R*" kept on sending ERROR messages instead of analyzing my data! And not forgetting, for the amazing time in Japan! Kampaiiiii! I am still laughing about the "at least you are loud"!

To Lei Cheng! Thanks for introducing me to Chinese culture! The green tea you bring from China is the best I have ever drunk. It brings back sharpness in working hours when it is difficult to concentrate! And thanks for telling me the right color of Fricke solution :)!

To Beata Brzozowska. Thanks for being adorable! I will always remember the movie you and the others made for me after my licentiate! I really enjoyed sharing the office with you! And what a hole you left when you went back to Poland! I missed your smile, your always positive attitude and organizing skills, and the way you simply explain the world with complicated equations! So happy you are here to attend my defense!

To Ayumi Nakamura, thanks for being the best guide and "dancing queen" in Japan! I never understood Karaoke before I met you! I admire your sense of hospitality and kindness!

To Traimate Sangsuwan. Tai, I still remember your words in my first week of working in the lab: "Do not worry! This week you are learning what to do

when things go wrong"! I will always be grateful for all the time you spent teaching me. And for taking care of my cat when we were away!

To Gunilla Olsson. Thanks for all the fun times together, it gives me good mood to spend time with you!

To Ali Pour Khavari, Paulo D'auria Vieira De Godoy, Alexandru Aanei, Pamela Akuwundike it has been really pleasant to work with you!

To all the members of the old radiobiology group: I have not forgotten you! Elina Staaf, Karl Brehwens, Eliana Beltran, Sara Skjöld, Sara Shakeri Manesh, Ainārs Bajinskis, Asal Fotouhi and Marina Ilic, it felt so lonely when you all graduated and just me and Tai were left in the lab!

And I would also like to thank Fredrik Hurtig for all the time spent together, discussing scientific projects, climbing or just drinking beer. Thanks for being a friend! Mattias Engelbrecht for the delicious cakes, for beer drinking and for cheering me up when my mood was down. Thanks for being a friend! Raquel Garcia Lobato Tavares a big thanks for all the time spent together! You are a great friend! Manuel Mata Forsberg, Andreas Ring, Mikaela Behm, Nele de Klerk, Carlotta Peselj, Jutta Diessl you made the pub evenings unforgettable! Jerker Eriksson thanks for sprängtickan! Stefanie Bauer thanks for the Monday-bread deliveries! Johan Seijsing for kayak pictures and interesting talks! A great thank goes also to the brave innebandy players! There is nothing like a dangerously high innebandy stick and a good laugh to take away the stress of the lab work!

Finally my last thanks goes to my family Marco and Giulia. You mean everything to me! Thanks for all the support, the delicious dinners prepared when I had to work late and for been always there for me! I love you!

Grazie anche a mia mamma Giovanna per essere sempre presente, per i "buon giorno" mattutini che mi hanno tenuto compagnia e hanno rischiarato ogni giornata buia! Ti voglio bene!

References

Ahnesorg P, Smith P, Jackson SP. 2006. XLF interacts with the XRCC4-DNA ligase IV complex to promote DNA nonhomologous end-joining. Cell 124(2):301-13.

Allen PD and Chaudhri M. 1988. Photoneutron production in tissue during high energy bremsstrahlung radiotherapy. Phys Med Biol 33(9):1017.

Anderson L, Henderson C, Adachi Y. 2001. Phosphorylation and rapid relocalization of 53BP1 to nuclear foci upon DNA damage. Mol Cell Biol 21(5):1719-29.

Ando K, Kernan JL, Liu PH, Sanda T, Logette E, Tschopp J, Look AT, Wang J, Bouchier-Hayes L, Sidi S. 2012. PIDD death-domain phosphorylation by ATM controls prodeath versus prosurvival PIDDosome signaling. Mol Cell 47(5):681-93.

Anheim M, Tranchant C, Koenig M. 2012. The autosomal recessive cerebellar ataxias. N Engl J Med 366(7):636-46.

Aten JA, Stap J, Krawczyk PM, van Oven CH, Hoebe RA, Essers J, Kanaar R. 2004. Dynamics of DNA double-strand breaks revealed by clustering of damaged chromosome domains. Science 303(5654):92-5.

Attix FH and Tochilin E. 2016. Sources, fields, measurements, and applications: Radiation dosimetry. Academic Press.

Bajinskis A, Natarajan AT, Erixon K, Harms-Ringdahl M. 2013. DNA double strand breaks induced by the indirect effect of radiation are more efficiently repaired by non-homologous end joining compared to homologous recombination repair. Mutation Research/Genetic Toxicology and Environmental Mutagenesis 756(1):21-9.

Baker M. 2010. Cellular imaging: Taking a long, hard look. Nature 466(7310):1137-40.

Bakkenist CJ and Kastan MB. 2003. DNA damage activates ATM through intermolecular autophosphorylation and dimer dissociation. Nature 421(6922):499-506.

Banda M, Bommineni A, Thomas RA, Luckinbill LS, Tucker JD. 2008. Evaluation and validation of housekeeping genes in response to ionizing radiation and chemical exposure for normalizing RNA expression in real-time PCR. Mutation Research/Genetic Toxicology and Environmental Mutagenesis 649(1–2):126-34.

Barak Y, Juven T, Haffner R, Oren M. 1993. Mdm2 expression is induced by wild type P53 activity. Embo J 12(2):461-8.

Barbui M., Hagel K., Gauthier J., Wuenschel S., Goldberg VZ, Zheng H., Giuliani G., Rapisarda G., Kim E-J and Liu X. 2015. Exploring clustering in alpha-conjugate nuclei using the thick target inverse kinematic technique for multiple alpha emission. APS division of nuclear physics meeting abstracts.

Barendsen G, Walter H, Fowler J, Bewley D. 1963. Effects of different ionizing radiations on human cells in tissue culture: III. experiments with cyclotron-accelerated alpha-particles and deuterons. Radiat Res 18(1):106-19.

Bayani J, Zielenska M, Pandita A, Al-Romaih K, Karaskova J, Harrison K, Bridge JA, Sorensen P, Thorner P, Squire JA. 2003. Spectral karyotyping identifies recurrent complex rearrangements of chromosomes 8, 17, and 20 in osteosarcomas. Genes, Chromosomes and Cancer 36(1):7-16.

Becker A, Durante M, Taucher-Scholz G, Jakob B. 2014. ATM alters the otherwise robust chromatin mobility at sites of DNA double-strand breaks (DSBs) in human cells. PloS One 9(3):e92640.

Bekker-Jensen S, Lukas C, Melander F, Bartek J, Lukas J. 2005. Dynamic assembly and sustained retention of 53BP1 at the sites of DNA damage are controlled by Mdc1/NFBD1. The Journal of Cell Biology 170(2):201-11.

Bennett PV, Cintron NS, Gros L, Laval J, Sutherland BM. 2004. Are endogenous clustered dna damages induced in human cells? Free Radical Biology and Medicine 37(4):488-99.

Berg HC. 1993. Random walks in biology. Princeton University Press.

Bieging KT, Mello SS, Attardi LD. 2014. Unravelling mechanisms of p53-mediated tumour suppression. Nat Rev Cancer 14(5):359-70.

Block WD, Yu Y, Merkle D, Gifford JL, Ding Q, Meek K, Lees-Miller SP. 2004. Autophosphorylation-dependent remodeling of the DNA-dependent protein kinase catalytic subunit regulates ligation of DNA ends. Nucleic Acids Research 32(14):4351-7.

Bornfleth H, Edelmann P, Zink D, Cremer T, Cremer C. 1999. Quantitative motion analysis of subchromosomal foci in living cells using four-dimensional microscopy. Biophys J 77(5):2871-86.

Bothmer A, Robbiani DF, Feldhahn N, Gazumyan A, Nussenzweig A, Nussenzweig MC. 2010. 53BP1 regulates DNA resection and the choice between classical and alternative end joining during class switch recombination. The Journal of Experimental Medicine 207(4):855-65.

Botuyan MV, Lee J, Ward IM, Kim J, Thompson JR, Chen J, Mer G. 2006. Structural basis for the methylation state-specific recognition of histone H4-K20 by 53BP1 and Crb2 in DNA repair. Cell 127(7):1361-73.

Bouwman P, Aly A, Escandell JM, Pieterse M, Bartkova J, van dG, Hiddingh S, Thanasoula M, Kulkarni A, Yang Q, et al. 2010. 53BP1 loss rescues BRCA1 deficiency and is associated with triple-negative and BRCA-mutated breast cancers. Nat Struct Mol Biol 17(6):688-95.

Brenner DJ and Hall EJ. 2008. Secondary neutrons in clinical proton radiotherapy: A charged issue. Radiotherapy and Oncology 86(2):165-70.

Brobeck WM, Lawrence E, MacKenzie K, McMillan E, Serber R, Sewell DC, Simpson K, Thornton R. 1947. Initial performance of the 184-inch cyclotron of the university of california. Physical Review 71(7):449.

Brooks AL, Newton GJ, Shyr L-, Seiler FA, Scott BR. 1990. The combined effects of α-particles and X-rays on cell killing and micronuclei induction in lung epithelial cells. Int J Radiat Biol 58(5):799-811.

Brown KE, Guest SS, Smale ST, Hahm K, Merkenschlager M, Fisher AG. 1997. Association of transcriptionally silent genes with ikaros complexes at centromeric heterochromatin. Cell 91(6):845-54.

Buck D, Malivert L, de Chasseval R, Barraud A, Fondanèche M, Sanal O, Plebani A, Stéphan J, Hufnagel M, le Deist F, et al. 2006. Cernunnos, a

novel nonhomologous end-joining factor, is mutated in human immunodeficiency with microcephaly. Cell 124(2):287-99.

Bunting SF, Callén E, Wong N, Chen H, Polato F, Gunn A, Bothmer A, Feldhahn N, Fernandez-Capetillo O, Cao L, et al. 2010. 53BP1 inhibits homologous recombination in Brca1-deficient cells by blocking resection of DNA breaks. Cell 141(2):243-54.

Burgkhardt B, Bilski P, Budzanowski M, Böttger R, Eberhardt K, Hampel G, Olko P, Straubing A. 2006. Application of different TL detectors for the photon dosimetry in mixed radiation fields used for BNCT. Radiat Prot Dosimet 120(1-4):83-6.

Burlinson B, Tice RR, Speit G, Agurell E, Brendler-Schwaab SY, Collins AR, Escobar P, Honma M, Kumaravel TS, Nakajima M. 2007. Fourth international workgroup on genotoxicity testing: Results of the in vivo comet assay workgroup. Mutation Research/Genetic Toxicology and Environmental Mutagenesis 627(1):31-5.

Cabal GG, Genovesio A, Rodriguez-Navarro S, Zimmer C, Gadal O, Lesne A, Buc H, Feuerbach-Fournier F, Olivo-Marin J, Hurt EC. 2006. SAGA interacting factors confine sub-diffusion of transcribed genes to the nuclear envelope. Nature 441(7094):770-3.

Cadet J and Davies KJ. 2017. Oxidative DNA damage & repair: An introduction. Free Radical Biology and Medicine .

Campos EI and Reinberg D. 2009. Histones: Annotating chromatin. Annu Rev Genet 43:559-99.

Ceccaldi R, Rondinelli B, D'Andrea AD. 2016. Repair pathway choices and consequences at the double-strand break. Trends Cell Biol 26(1):52-64.

Chakraborty A, Tapryal N, Venkova T, Horikoshi N, Pandita RK, Sarker AH, Sarkar PS, Pandita TK, Hazra TK. 2016. Classical non-homologous end-joining pathway utilizes nascent RNA for error-free double-strand break repair of transcribed genes. Nat Commun 7:13049.

Chan DW, Chen BP, Prithivirajsingh S, Kurimasa A, Story MD, Qin J, Chen DJ. 2002. Autophosphorylation of the DNA-dependent protein kinase catalytic subunit is required for rejoining of DNA double-strand breaks. Genes & Development 16(18):2333-8.

Chapman J , Taylor MG, Boulton S. 2012. Playing the end game: DNA double-strand break repair pathway choice. Mol Cell 47(4):497-510.

Chen Z, Yang H, Pavletich NP. 2008. Mechanism of homologous recombination from the RecA-ssDNA/dsDNA structures. Nature 453(7194):489-94.

Chiolo I, Tang J, Georgescu W, Costes SV. 2013. Nuclear dynamics of radiation-induced foci in euchromatin and heterochromatin. Mutation Research/Fundamental and Molecular Mechanisms of Mutagenesis 750(1):56-66.

Chubb JR, Boyle S, Perry P, Bickmore WA. 2002. Chromatin motion is constrained by association with nuclear compartments in human cells. Current Biology 12(6):439-45.

Collins AR. 2004. The comet assay for DNA damage and repair. Mol Biotechnol 26(3):249.

Collis SJ, DeWeese TL, Jeggo PA, Parker AR. 2004. The life and death of DNA-PK. Oncogene 24(6):949-61.

Costantini S, Woodbine L, Andreoli L, Jeggo PA, Vindigni A. 2007. Interaction of the ku heterodimer with the DNA ligase IV/Xrcc4 complex and its regulation by DNA-PK. DNA Repair 6(6):712-22.

Costes SV, Boissière A, Ravani S, Romano R, Parvin B, Barcellos-Hoff MH. 2006. Imaging features that discriminate between foci induced by high-and low-LET radiation in human fibroblasts. Radiat Res 165(5):505-15.

Crawley MJ. 2012. The R book. John Wiley & Sons.

Cucinotta FA. 2015. Review of NASA approach to space radiation risk assessments for mars exploration. Health Phys 108(2):131-42.

Cucinotta FA, Kim MY, Chappell LJ, Huff JL. 2013. How safe is safe enough? radiation risk for a human mission to mars. PLoS ONE 8(10):e74988.

Cuella-Martin R, Oliveira C, Lockstone HE, Snellenberg S, Grolmusova N, Chapman JR. 2016. 53BP1 integrates DNA repair and p53-dependent cell fate decisions via distinct mechanisms. Mol Cell 64(1):51-64.

Dahm K. 2007. Functions and regulation of human artemis in double strand break repair. J Cell Biochem 100(6):1346-51.

Danovi D, Meulmeester E, Pasini D, Migliorini D, Capra M, Frenk R, de Graaf P, Francoz S, Gasparini P, Gobbi A, et al. 2004. Amplification of mdmx (or Mdm4) directly contributes to tumor formation by inhibiting p53 tumor suppressor activity. Mol Cell Biol 24(13):5835-43.

Datta K, Neumann RD, Winters TA. 2005. Characterization of complex apurinic/apyrimidinic-site clustering associated with an authentic site-specific radiation-induced DNA double-strand break. Proceedings of the National Academy of Sciences of the United States of America 102(30):10569-74.

De Bont R and Van Larebeke N. 2004. Endogenous DNA damage in humans: A review of quantitative data. Mutagenesis 19(3):169-85.

DeFazio LG, Stansel RM, Griffith JD, Chu G. 2002. Synapsis of DNA ends by DNA-dependent protein kinase. Embo J 21(12):3192-200.

Demizu Y, Kagawa K, Ejima Y, Nishimura H, Sasaki R, Soejima T, Yanou T, Shimizu M, Furusawa Y, Hishikawa Y, et al. 2004. Cell biological basis for combination radiotherapy using heavy-ion beams and high-energy X-rays. Radiotherapy and Oncology 71(2):207-11.

Dextraze M, Gantchev T, Girouard S, Hunting D. 2010. DNA interstrand cross-links induced by ionizing radiation: An unsung lesion. Mutation Research/Reviews in Mutation Research 704(1–3):101-7.

Difilippantonio MJ, Zhu J, Chen HT, Meffre E, Nussenzweig MC, Max EE, Ried T, Nussenzweig A. 2000. DNA repair protein Ku80 suppresses chromosomal aberrations and malignant transformation. Nature 404(6777):510-4.

Dimitrova N, Chen YM, Spector DL, de Lange T. 2008. 53BP1 promotes non-homologous end joining of telomeres by increasing chromatin mobility. Nature 456(7221):524-8.

Dion V and Gasser SM. 2013. Chromatin movement in the maintenance of genome stability. Cell 152(6):1355-64.

Dizdaroglu M. 1992. Oxidative damage to DNA in mammalian chromatin. Mutation Research/DNAging 275(3):331-42.

Duarte V, Muller JG, Burrows CJ. 1999. Insertion of dGMP and dAMP during in vitro DNA synthesis opposite an oxidized form of 7,8-dihydro-8-oxoguanine. Nucleic Acids Res 27(2):496-502.

Durocher D and Pelletier L. 2016. 53BP1 goes back to its p53 roots. Mol Cell 64(1):3-4.

Eberharter A and Becker PB. 2002. Histone acetylation: A switch between repressive and permissive chromatin. second in review series on chromatin dynamics. EMBO Rep 3(3):224-9.

Eccles LJ, Lomax ME, O'Neill P. 2009. Hierarchy of lesion processing governs the repair, double-strand break formation and mutability of three-lesion clustered DNA damage. Nucleic Acids Res 38(4):1123-34.

Ettinger A and Wittmann T. 2014. Fluorescence live cell imaging. Methods Cell Biol 123:77-94.

Falk M, Lukasova E, Gabrielova B, Ondrej V, Kozubek S. 2007. Chromatin dynamics during DSB repair. Biochimica Et Biophysica Acta (BBA)-Molecular Cell Research 1773(10):1534-45.

Falk M, Lukasova E, Kozubek S. 2010. Higher-order chromatin structure in DSB induction, repair and misrepair. Mutation Research/Reviews in Mutation Research 704(1–3):88-100.

Falk M, Lukášová E, Kozubek S. 2008. Chromatin structure influences the sensitivity of DNA to γ-radiation. Biochimica Et Biophysica Acta (BBA) - Molecular Cell Research 1783(12):2398-414.

Ferguson Lynnette R., Chen Helen, Collins Andrew R., Connell Marisa, Damia Giovanna, Dasgupta Santanu, Malhotra Meenakshi, Meeker Alan K., Amedei Amedeo and Amin Amr. 2015. Genomic instability in human cancer: Molecular insights and opportunities for therapeutic attack and prevention through diet and nutrition. Seminars in cancer biologyElsevier. S5 p.

Fotouhi A, Skiöld S, Shakeri-Manesh S, Osterman-Golkar S, Wojcik A, Jenssen D, Harms-Ringdahl M, Haghdoost S. 2011. Reduction of 8-oxodGTP in the nucleotide pool by hMTH1 leads to reduction in mutations in the human lymphoblastoid cell line TK6 exposed to UVA. Mutation Research/Fundamental and Molecular Mechanisms of Mutagenesis 715(1–2):13-8.

Fradet-Turcotte,Amelie, Canny M,D., Escribano-Diaz,Cristina, Orthwein,Alexandre, Leung CC,Y., Huang,Hao, Landry,Marie-Claude, Kitevski-LeBlanc,Julianne, Noordermeer S,M., Sicheri,Frank, et al. 2013. 53BP1 is a reader of the DNA-damage-induced H2A lys 15 ubiquitin mark. Nature (499):50–54.

Francis Z, Incerti S, Karamitros M, Tran HN, Villagrasa C. 2011. Stopping power and ranges of electrons, protons and alpha particles in liquid water using the Geant4-DNA package. Nuclear Instruments and Methods in Physics Research Section B: Beam Interactions with Materials and Atoms 269(20):2307-11.

Friedberg EC, Walker GR, Siede W, Wood RD, Schults R, A., Ellenberger T. 2006. Base excision repair. In: DNA repair and mutagenesis. second ed. ASM press. 169-226 p.

Fu D, Calvo JA, Samson LD. 2012. Balancing repair and tolerance of DNA damage caused by alkylating agents. Nat Rev Cancer 12(2):104-20.

Furth EE, Thilly WG, Penman BW, Liber HL, Rand WM. 1981. Quantitative assay for mutation in diploid human lymphoblasts using microtiter plates. Anal Biochem 110(1):1-8.

Furusawa Y, Aoki M, Durante M. 2002. Simultaneous exposure of mammalian cells to heavy ions and X-rays. Advances in Space Research 30(4):877-84.

Gad S. 2008. Protocols for in vitro mammalian cell mutation assay. In: Preclinical development handbook: Toxicology. Shayne Cox Gad, editor. New Jersey: John Wiley and Sons, Inc, Publication. 132-153 p.

Gaglia G, Guan Y, Shah JV, Lahav G. 2013. Activation and control of p53 tetramerization in individual living cells. Proc Natl Acad Sci U S A 110(38):15497-501.

Gell D and Jackson SP. 1999. Mapping of protein-protein interactions within the DNA-dependent protein kinase complex. Nucleic Acids Research 27(17):3494-502.

Georgakilas AG, Bennett PV, Wilson III DM, Sutherland BM. 2004. Processing of bistranded abasic DNA clusters in γ-irradiated human hematopoietic cells. Nucleic Acids Res 32(18):5609-20.

Georgakilas AG, O'Neill P, Stewart RD. 2013. Induction and repair of clustered DNA lesions: What do we know so far? Radiat Res 180(1):100-9.

Gilley D, Tanaka H, Hande MP, Kurimasa A, Li GC, Oshimura M, Chen DJ. 2001. DNA-PKcs is critical for telomere capping. Proc Natl Acad Sci U S A 98(26):15084-8.

Girst S, Hable V, Drexler G, Greubel C, Siebenwirth C, Haum M, Friedl A, Dollinger G. 2013. Subdiffusion supports joining of correct ends during repair of DNA double-strand breaks. Scientific Reports 3:2511.

Gollapalle E, Wang R, Adetolu R, Tsao D, Francisco D, Sigounas G, Georgakilas AG. 2007. Detection of oxidative clustered DNA lesions in X-irradiated mouse skin tissues and human MCF-7 breast cancer cells. Radiat Res 167(2):207-16.

Goodhead D. 1995. Molecular and cell models of biological effects of heavy ion radiation. Radiat Environ Biophys 34(2):67-72.

Goodhead DT. 1992. Track structure considerations in low dose and low dose rate effects of ionizing radiation. Adv Radiat Biol 16:7-44.

Goodhead DT. 1994. Initial events in the cellular effects of ionizing radiations: Clustered damage in DNA. Int J Radiat Biol 65(1):7-17.

Goodhead DT, Thacker J, Cox R. 1993. Effects of radiations of different qualities on cells: Molecular mechanisms of damage and repair. Int J Radiat Biol 63(5):543-56.

Greubel C, Hable V, Drexler GA, Hauptner A, Dietzel S, Strickfaden H, Baur I, Krücken R, Cremer T, Dollinger G. 2008. Competition effect in DNA damage response. Radiat Environ Biophys 47(4):423-9.

Grewal SI and Moazed D. 2003. Heterochromatin and epigenetic control of gene expression. Science 301(5634):798-802.

Gu J, Lu H, Tippin B, Shimazaki N, Goodman MF, Lieber MR. 2007. XRCC4:DNA ligase IV can ligate incompatible DNA ends and can ligate across gaps. Embo J 26(4):1010-23.

Gulston M, de Lara C, Jenner T, Davis E, O'Neill P. 2004. Processing of clustered DNA damage generates additional double-strand breaks in mammalian cells post-irradiation. Nucleic Acids Res 32(4):1602-9.

Hable V, Drexler GA, Brüning T, Burgdorf C, Greubel C, Derer A, Seel J, Strickfaden H, Cremer T, Friedl AA. 2012. Recruitment kinetics of DNA repair proteins Mdc1 and Rad52 but not 53BP1 depend on damage complexity. PloS One 7(7):e41943.

Hall E and Giaccia J. 2012a. Cell, tissue, and tumor kinetics. Radiobiology for the Radiologist, 7th Ed.Lippincott Williams & Wilkins, Philadelphia :372-90.

Hall EJ and Giaccia AJ. 2012b. Radiobiology for the radiologist. seventh edition ed. Philadelpha: Wolters Kluwer-Lippincott Williams & Wilkins.

Halliwell B and Gutteridge JM. 2015. Free radicals in biology and medicine. Oxford University Press, USA.

Harrigan JA, Belotserkovskaya R, Coates J, Dimitrova DS, Polo SE, Bradshaw CR, Fraser P, Jackson SP. 2011. Replication stress induces 53BP1-containing OPT domains in G1 cells. The Journal of Cell Biology 193(1):97-108.

Harris CC and Hollstein M. 1993. Clinical implications of the p53 tumor-suppressor gene. N Engl J Med 329(18):1318-27.

Hartley KO, Gell D, Smith GCM, Zhang H, Divecha N, Connelly MA, Admon A, Lees-Miller S, Anderson CW, Jackson SP. 1995. DNA-dependent protein kinase catalytic subunit: A relative of phosphatidylinositol 3-kinase and the ataxia telangiectasia gene product. Cell 82(5):849-56.

Hashimoto K, Tominaga Y, Nakabeppu Y, Moriya M. 2004. Futile short-patch DNA base excision repair of adenine:8-oxoguanine mispair. Nucleic Acids Research 32(19):5928-34.

Hawley BR, Lu W, Wilczynska A, Bushell M. 2017. The emerging role of RNAs in DNA damage repair. Cell Death & Differentiation 24(4):580-7.

Heun P, Laroche T, Shimada K, Furrer P, Gasser SM. 2001. Chromosome dynamics in the yeast interphase nucleus. Science 294(5549):2181-6.

Hickman MJ and Samson LD. 1999. Role of DNA mismatch repair and p53 in signaling induction of apoptosis by alkylating agents. Proc Natl Acad Sci U S A 96(19):10764-9.

Hill M. 1999. Radiation damage to DNA: The importance of track structure. Radiat Measur 31(1):15-23.

Hlatky L. 2012. Double-strand break motions shift radiation risk notions? Proc Natl Acad Sci U S A 109(2):351-2.

Hoeijmakers JH. 2001. Genome maintenance mechanisms for preventing cancer. Nature 411(6835):366.

Holliday R. 1964. A mechanism for gene conversion in fungi. Genetics Research 5(02):282-304.

Honda R, Tanaka H, Yasuda H. 1997. Oncoprotein MDM2 is a ubiquitin ligase E3 for tumor suppressor p53. FEBS Lett 420(1):25-7.

Hornik K. 2012. The comprehensive R archive network. Wiley Interdisciplinary Reviews: Computational Statistics 4(4):394-8.

Horowitz YS. 2006. A unified and comprhensive theory of the TL dose response of thermoluminescent systems applied to LiF:Mg, ti. In: Microdosimetric response of physical and biological systems to low and high-LET radiatios. First edition ed. Elsevier. 77-82 p.

Hu Y, Wang C, Huang K, Xia F, Parvin JD, Mondal N. 2014. Regulation of 53BP1 protein stability by RNF8 and RNF168 is important for efficient DNA double-strand break repair. PloS One 9(10):e110522.

Huen MS, Grant R, Manke I, Minn K, Yu X, Yaffe MB, Chen J. 2007. RNF8 transduces the DNA-damage signal via histone ubiquitylation and checkpoint protein assembly. Cell 131(5):901-14.

Hustedt N and Durocher D. 2017. The control of DNA repair by the cell cycle. Nat Cell Biol 19(1):1-9.

International Commission on Radiological Protection. 1991. ICRP publication 60: 1990 recommendations of the international commission on radiological protection. Elsevier Health Sciences.

Isabelle V, Prévost C, Spotheim-Maurizot M, Sabattier R, Charlier M. 1995. Radiation-induced damages in single- and double-stranded DNA. Int J Radiat Biol 67(2):169-76.

Isfort RJ, Cody DB, Lovell G, Doersen C. 1995. Analysis of oncogenes, tumor suppressor genes, autocrine growth-factor production, and differentiation state of human osteosarcoma cell lines. Mol Carcinog 14(3):170-8.

Isono M, Niimi A, Oike T, Hagiwara Y, Sato H, Sekine R, Yoshida Y, Isobe S, Obuse C, Nishi R. 2017. BRCA1 directs the repair pathway to homologous recombination by promoting 53BP1 dephosphorylation. Cell Reports 18(2):520-32.

Iwabuchi K, Bartel PL, Li B, Marraccino R, Fields S. 1994. Two cellular proteins that bind to wild-type but not mutant p53. Proceedings of the National Academy of Sciences 91(13):6098-102.

Jakob B, Splinter J, Taucher-Scholz G. 2009. Positional stability of damaged chromatin domains along radiation tracks in mammalian cells. Radiat Res 171(4):405-18.

Jakob B, Splinter J, Durante M, Taucher-Scholz G. 2009. Live cell microscopy analysis of radiation-induced DNA double-strand break motion. Proceedings of the National Academy of Sciences 106(9):3172-7.

Jakob B, Rudolph JH, Gueven N, Lavin MF, Taucher-Scholz G. 2005. Live cell imaging of heavy-ion-induced radiation responses by beamline microscopy. Radiat Res 163(6):681-90.

Jakob B, Splinter J, Conrad S, Voss KO, Zink D, Durante M, Lobrich M, Taucher-Scholz G. 2011. DNA double-strand breaks in heterochromatin elicit fast repair protein recruitment, histone H2AX phosphorylation and relocation to euchromatin. Nucleic Acids Res 39(15):6489-99.

Jasin M and Rothstein R. 2013. Repair of strand breaks by homologous recombination. Cold Spring Harbor Perspectives in Biology 5(11).

Jeggo P. 1998. Identification of genes involved in repair of DNA double-strand breaks in mammalian cells. Radiat Res 150(5s):S80-91.

Joiner M and vand der Kogel A, editors. 2009. Basic clinical radiobiology. Fourth Edition ed. Great Britain: Hodder Arnold.

Jones S, Emmerson P, Maynard J, Best JM, Jordan S, Williams GT, Sampson JR, Cheadle JP. 2002. Biallelic germline mutations in MYH predispose to multiple colorectal adenoma and somatic G:C→T:A mutations. Human Molecular Genetics 11(23):2961-7.

Karger C and Oliver J. 2007. Current status and new developments in ion therapy. Strahlentherapie Und Onkologie 183(6).

Khalil H, Tummala H, Zhelev N. 2012. ATM in focus: A damage sensor and cancer target. Biodiscovery 5.

Kim MS, Blake M, Baek JH, Kohlhagen G, Pommier Y, Carrier F. 2003. Inhibition of histone deacetylase increases cytotoxicity to anticancer drugs targeting DNA. Cancer Res 63(21):7291-300.

Kinney NA, Onufriev AV, Sharakhov IV. 2015. Quantified effects of chromosome-nuclear envelope attachments on 3D organization of chromosomes. Nucleus 6(3):212-24.

Kraft G and Scholz M. 1994. On the parametrization of the biological effect in a mixed radiation field. Advances in Space Research 14(10):997-1004.

Krejci L, Altmannova V, Spirek M, Zhao X. 2012. Homologous recombination and its regulation. Nucleic Acids Research 40(13):5795-818.

Kronenberg A and Little JB. 1989. Locus specificity for mutation induction in human cells exposed to accelerated heavy ions. Int J Radiat Biol 55(6):913-24.

Kruhlak MJ, Celeste A, Dellaire G, Fernandez-Capetillo O, Muller WG, McNally JG, Bazett-Jones DP, Nussenzweig A. 2006a. Changes in chromatin structure and mobility in living cells at sites of DNA double-strand breaks. J Cell Biol 172(6):823-34.

Kruhlak MJ, Celeste A, Dellaire G, Fernandez-Capetillo O, Muller WG, McNally JG, Bazett-Jones DP, Nussenzweig A. 2006b. Changes in chromatin structure and mobility in living cells at sites of DNA double-strand breaks. J Cell Biol 172(6):823-34.

Kruhlak MJ, Celeste A, Dellaire G, Fernandez-Capetillo O, MÃ¼ller W,G., McNally JG, Bazett-Jones D, Nussenzweig A. 2006c. Changes in chromatin structure and mobility in living cells at sites of DNA double-strand breaks. J Cell Biol 172(6):823-34.

Laramore GE, Liao JJ, Rockhill JK, Komarnicky-Kocher L. 2013. Relative biological effectiveness (RBE). In: Encyclopedia of radiation oncology. Brady LW and Yaeger TE, editors. Berlin, Heidelberg: Springer Berlin Heidelberg. 748 p.

Lavelle C and Foray N. 2014. Chromatin structure and radiation-induced DNA damage: From structural biology to radiobiology. Int J Biochem Cell Biol 49:84-97.

Lebeaupin T, Sellou H, Timinszky G, Huet S. 2015. Chromatin dynamics at DNA breaks: What, how and why? AIMS Biophysics 2:458-75.

Lee J and Paull TT. 2004. Direct activation of the ATM protein kinase by the Mre11/Rad50/Nbs1 complex. Science 304(5667):93-6.

Leuther KK, Hammarsten O, Kornberg RD, Chu G. 1999. Structure of DNA-dependent protein kinase: Implications for its regulation by DNA. Embo J 18(5):1114-23.

Lieberman-Aiden E, van Berkum NL, Williams L, Imakaev M, Ragoczy T, Telling A, Amit I, Lajoie BR, Sabo PJ, Dorschner MO, et al. 2009. Comprehensive mapping of long-range interactions reveals folding principles of the human genome. Science 326(5950):289-93.

Lindahl T. 1993. Instability and decay of the primary structure of DNA. Nature 362(6422):709-15.

Little J, Nagasawa H, Keng P, Yu Y, Li C. 1995. Absence of radiation-induced G1 arrest in two closely related human lymphoblast cell lines that differ in p53 status. Journal of Biological Chemistry 270(19):11033-6.

Liu Y, Cussiol JR, Dibitetto D, Sims JR, Twayana S, Weiss RS, Freire R, Marini F, Pellicioli A, Smolka MB. 2017. TOPBP1Dpb11 plays a conserved role in homologous recombination DNA repair through the coordinated recruitment of 53BP1Rad9. J Cell Biol 216(3):623-39.

Liu Z, Liu Q, Xu B, Wu J, Guo C, Zhu F, Yang Q, Gao G, Gong Y, Shao C. 2009. Berberine induces p53-dependent cell cycle arrest and apoptosis of human osteosarcoma cells by inflicting DNA damage. Mutation Research/Fundamental and Molecular Mechanisms of Mutagenesis 662(1–2):75-83.

Lodish H, Berk A, Zipursky Sl, Matsudaria P, Baltimore D, Darnell J. 2000. Molecular cell biology. fourth edition ed. W.H. Freeman and Company.

Lomax ME, Salje H, Cunniffe S, O'Neill P. 2005. 8-OxoA inhibits the incision of an AP site by the DNA glycosylases fpg, nth and the AP endonuclease HAP1. Radiat Res 163(1):79-84.

Lorat Y, Brunner CU, Schanz S, Jakob B, Taucher-Scholz G, Rübe CE. 2015. Nanoscale analysis of clustered DNA damage after high-LET irradiation by quantitative electron microscopy–the heavy burden to repair. DNA Repair 28:93-106.

Lottersberger F, Karssemeijer RA, Dimitrova N, de Lange T. 2015. 53BP1 and the LINC complex promote microtubule-dependent DSB mobility and DNA repair. Cell 163(4):880-93.

Lukas,Claudia, Savic,Velibor, Bekker-Jensen,Simon, Doil,Carsten, Neumann,Beate, Solvhoj Pedersen,Ronni, Grofte,Merete, Chan K,Lung, Hickson I,David, Bartek,Jiri, et al. 53BP1 nuclear bodies form around DNA lesions generated by mitotic transmission of chromosomes under replication stress. .

Lukas C, Falck J, Bartkova J, Bartek J, Lukas J. 2003. Distinct spatiotemporal dynamics of mammalian checkpoint regulators induced by DNA damage. Nat Cell Biol 5(3):255-60.

Maeda A, Chen Y, Bu J, Mujcic H, Wouters BG, DaCosta RS. 2017. In vivo imaging reveals significant tumor vascular dysfunction and increased tumor hypoxia-inducible factor-1α expression induced by high single-dose irradiation in a pancreatic tumor model. International Journal of Radiation Oncology* Biology* Physics 97(1):184-94.

Maltzman W and Czyzyk L. 1984. UV irradiation stimulates levels of p53 cellular tumor antigen in nontransformed mouse cells. Molecular and Cellular Biology 4(9):1689-94.

Manis JP, Morales JC, Xia Z, Kutok JL, Alt FW, Carpenter PB. 2004. 53BP1 links DNA damage-response pathways to immunoglobulin heavy chain class-switch recombination. Nat Immunol 5(5):481-7.

Mari P, Florea BI, Persengiev SP, Verkaik NS, Brüggenwirth HT, Modesti M, Giglia-Mari G, Bezstarosti K, Demmers JAA, Luider TM, et al. 2006. Dynamic assembly of end-joining complexes requires interaction between Ku70/80 and XRCC4. Proceedings of the National Academy of Sciences 103(49):18597-602.

Markova E, Schultz N, Belyaev I. 2007. Kinetics and dose-response of residual 53BP1/γ-H2AX foci: Co-localization, relationship with DSB repair and clonogenic survival. Int J Radiat Biol 83(5):319-29.

Marshall W, Straight A, Marko J, Swedlow J, Dernburg A, Belmont A, Murray A, Agard D, Sedat J. 1997. Interphase chromosomes undergo constrained diffusional motion in living cells. Current Biology 7(12):930-9.

Martin CJ and Sutton DG. 2015. Practical radiation protection in healthcare. second edition ed. Oxdord, UK: Oxford university press.

Mason AJ, Giusti V, Green S, af Rosenschöld PM, Beynon TD, Hopewell JW. 2011. Interaction between the biological effects of high-and low-LET radiation dose components in a mixed field exposure. Int J Radiat Biol 87(12):1162-72.

Mayer S, Forkel-Wirth D, Fuerstner M, Menzel H, Mueller M, Perrin D, Theis C, Vincke H. 2007. Response of neutron detectors to high-energy mixed radiation fields. Radiat Prot Dosimet 125(1-4):289-92.

Mazzei F, Viel A, Bignami M. 2013. Role of MUTYH in human cancer. Mutation Research/Fundamental and Molecular Mechanisms of Mutagenesis 743:33-43.

McNair A, Glover R, Wilson H. 1956. XVIII. the decay of potassium 40. Philosophical Magazine 1(2):199-211.

McNally NJ, de Ronde J, Folkard M. 1988. Interaction between X-ray and α-particle damage in V79 cells. Int J Radiat Biol 53(6):917-20.

McNally NJ, de Ronde J, Hinchliffe M. 1984. The effect of sequential irradiation with X-rays and fast neutrons on the survival of V79 chinese hamster cells. International Journal of Radiation Biology and Related Studies in Physics, Chemistry and Medicine 45(4):301-10.

Meisberger LL, Keller RJ, Shalek RJ. 1968. The effective attenuation in water of the gamma rays of gold 198, iridium 192, cesium 137, radium 226, and cobalt 60. Radiology 90(5):953-7.

Miller EC and Miller JA. 1981. Mechanisms of chemical carcinogenesis. Cancer 47(S5):1055-64.

Miné J, Disseau L, Takahashi M, Cappello G, Dutreix M, Viovy J. 2007. Real-time measurements of the nucleation, growth and dissociation of single Rad51–DNA nucleoprotein filaments. Nucleic Acids Research 35(21):7171-87.

Miné-Hattab J and Rothstein R. 2012. Increased chromosome mobility facilitates homology search during recombination. Nat Cell Biol 14(5):510.

Mochan TA, Venere M, DiTullio RA, Halazonetis TD. 2003. 53BP1 and NFBD1/MDC1-Nbs1 function in parallel interacting pathways activating ataxia-telangiectasia mutated (ATM) in response to DNA damage. Cancer Research 63(24):8586-91.

Momand J, Zambetti GP, Olson DC, George D, Levine AJ. 1992. The mdm-2 oncogene product forms a complex with the p53 protein and inhibits p53-mediated transactivation. Cell 69(7):1237-45.

Moriya M and Grollman AP. 1993. Mutations in the mutY gene of escherichia coli enhance the frequency of targeted G: C→ T: A transversions induced by a single 8-oxoguanine residue in single-stranded DNA. Molecular and General Genetics MGG 239(1-2):72-6.

Neumaier T, Swenson J, Pham C, Polyzos A, Lo AT, Yang P, Dyball J, Asaithamby A, Chen DJ, Bissell MJ, et al. 2012. Evidence for formation of DNA repair centers and dose-response nonlinearity in human cells. Proc Natl Acad Sci U S A 109(2):443-8.

Neumann FR, Dion V, Gehlen LR, Tsai-Pflugfelder M, Schmid R, Taddei A, Gasser SM. 2012. Targeted INO80 enhances subnuclear chromatin movement and ectopic homologous recombination. Genes Dev 26(4):369-83.

Ngo FQH, Blakely EA, Tobias CA. 1981. Sequential exposures of mammalian cells to low- and high-LET radiations: I. lethal effects following X-ray and neon-ion irradiation. Radiat Res 87(1):59-78.

Niforou KM, Anagnostopoulos AK, Vougas K, Kittas C, Gorgoulis VG, Tsangaris GT. 2008. The proteome profile of the human osteosarcoma U2OS cell line. Cancer Genomics Proteomics 5(1):63-78.

Nikitaki Z, Nikolov V, Mavragani IV, Plante I, Emfietzoglou D, Iliakis G, Georgakilas AG. 2016a. Non-DSB clustered DNA lesions. does theory colocalize with the experiment? Radiat Phys Chem 128:26-35.

Nikitaki Z, Nikolov V, Mavragani IV, Mladenov E, Mangelis A, Laskaratou DA, Fragkoulis GI, Hellweg CE, Martin OA, Emfietzoglou D. 2016b. Measurement of complex DNA damage induction and repair in human cellular systems after exposure to ionizing radiations of varying linear energy transfer (LET). Free Radic Res 50(sup1):S64-78.

Nikjoo H, O'Neill P, Terrissol M, Goodhead DT. 1999. Quantitative modelling of DNA damage using monte carlo track structure method. Radiat Environ Biophys 38(1):31-8.

Noon AT, Shibata A, Rief N, Lobrich M, Stewart GS, Jeggo PA, Goodarzi AA. 2010. 53BP1-dependent robust localized KAP-1 phosphorylation is essential for heterochromatic DNA double-strand break repair. Nat Cell Biol 12(2):177-84.

Nygren J, Ljungman M, Ahnström M. 1995. Chromatin structure and radiation-induced DNA strand breaks in human cells: Soluble scavengers and DNA-bound proteins offer a better protection against single-than double-strand breaks. Int J Radiat Biol 68(1):11-8.

Ochs F, Somyajit K, Altmeyer M, Rask M, Lukas J, Lukas C. 2016. 53BP1 fosters fidelity of homology-directed DNA repair. Nature Structural & Molecular Biology .

OECD. 1997. Test no. 476: In vitro mammalian cell gene mutation test. Organisation for Economic Co-operation and Development.

Ogawa T, Yu X, Shinohara A, Egelman E. 1993. Similarity of the yeast RAD51 filament to the bacterial RecA filament. Science 259(5103):1896-9.

Ohashi E, Takeishi Y, Ueda S, Tsurimoto T. 2014. Interaction between Rad9–Hus1–Rad1 and TopBP1 activates ATR–ATRIP and promotes TopBP1 recruitment to sites of UV-damage. DNA Repair 21:1-11.

Oka S and Nakabeppu Y. 2011. DNA glycosylase encoded by MUTYH functions as a molecular switch for programmed cell death under oxidative stress to suppress tumorigenesis. Cancer Science 102(4):677-82.

Oliner JD, Pietenpol JA, Thiagalingam S, Gyuris J, Kinzler KW, Vogelstein B. 1993. Oncoprotein MDM2 conceals the activation domain of tumour suppressor p53. Nature 362(6423):857.

Paap B, Wilson III DM, Sutherland BM. 2008. Human abasic endonuclease action on multilesion abasic clusters: Implications for radiation-induced biological damage. Nucleic Acids Res 36(8):2717-27.

Pandita TK, Lieberman HB, Lim DS, Dhar S, Zheng W, Taya Y, Kastan MB. 2000. Ionizing radiation activates the ATM kinase throughout the cell cycle. Oncogene 19(11):1386-91.

Paull TT. 2015. Mechanisms of ATM activation. Annu Rev Biochem 84(1):711-38.

Petitjean A, Achatz MIW, Borresen-Dale A, Hainaut P, Olivier M. 2007. TP53 mutations in human cancers: Functional selection and impact on cancer prognosis and outcomes. Oncogene 26(15):2157-65.

Petukhova G, Stratton S, Sung P. 1998. Catalysis of homologous DNA pairing by yeast Rad51 and Rad54 proteins. Nature 393(6680):91-4.

Phoenix B, Green S, Hill MA, Jones B, Mill A, Stevens DL. 2009. Do the various radiations present in BNCT act synergistically? cell survival experiments in mixed alpha-particle and gamma-ray fields. Applied Radiation and Isotopes 67(7–8, Supplement):S318-20.

Ponten J and Saksela E. 1967. Two established in vitro cell lines from human mesenchymal tumours. International Journal of Cancer 2(5):434-47.

Povirk LF and Finley Austin MJ. 1991. Genotoxicity of bleomycin. Mutation Research/Reviews in Genetic Toxicology 257(2):127-43.

Radicella JP, Dherin C, Desmaze C, Fox MS, Boiteux S. 1997. Cloning and characterization of hOGG1, a human homolog of the OGG1 gene of saccharomyces cerevisiae. Proc Natl Acad Sci U S A 94(15):8010-5.

Rafnsson V, Olafsdottir E, Hrafnkelsson J, Sasaki H, Arnarsson A, Jonasson F. 2005. Cosmic radiation increases the risk of nuclear cataract in airline pilots: A population-based case-control study. Arch Ophthalmol 123(8):1102-5.

Railton R, Lawson RC, Porter D. 1975. Interaction of γ-ray and neutron effects on the proliferative capacity of chinese hamster cells. International Journal of Radiation Biology and Related Studies in Physics, Chemistry and Medicine 27(1):75-82.

Rall M, Kraft D, Volcic M, Cucu A, Nasonova E, Taucher-Scholz G, Bonig H, Wiesmuller L, Fournier C. 2015. Impact of charged particle exposure on homologous DNA double-strand break repair in human blood-derived cells. Front Oncol 5:250.

Rao SS, Huntley MH, Durand NC, Stamenova EK, Bochkov ID, Robinson JT, Sanborn AL, Machol I, Omer AD, Lander ES. 2014. A 3D map of

the human genome at kilobase resolution reveals principles of chromatin looping. Cell 159(7):1665-80.

Rappold I, Iwabuchi K, Date T, Chen J. 2001. Tumor suppressor P53 binding protein 1 (53bp1) is involved in DNA Damage–Signaling pathways. The Journal of Cell Biology 153(3):613-20.

Ravanat J, Breton J, Douki T, Gasparutto D, Grand A, Rachidi W, Sauvaigo S. 2014. Radiation-mediated formation of complex damage to DNA: A chemical aspect overview. Br J Radiol 87(1035):20130715.

Regulus P, Duroux B, Bayle P, Favier A, Cadet J, Ravanat J. 2007. Oxidation of the sugar moiety of DNA by ionizing radiation or bleomycin could induce the formation of a cluster DNA lesion. Proceedings of the National Academy of Sciences 104(35):14032-7.

Reindl J, Girst S, Walsh DW, Greubel C, Schwarz B, Siebenwirth C, Drexler GA, Friedl AA, Dollinger G. 2017. Chromatin organization revealed by nanostructure of irradiation induced γH2AX, 53BP1 and Rad51 foci. Scientific Reports 7:40616.

Riley T, Sontag E, Chen P, Levine A. 2008. Transcriptional control of human p53-regulated genes. Nat Rev Mol Cell Biol 9(5):402-12.

Robertson AB, Klungland A, Rognes T, Leiros I. 2009. DNA repair in mammalian cells. Cellular and Molecular Life Sciences 66(6):981-93.

Roos WP, Thomas AD, Kaina B. 2016. DNA damage and the balance between survival and death in cancer biology. Nature Reviews Cancer 16(1):20-33.

Ruggieri V, Pin E, Russo M, Barone F, Degan P, Sanchez M, Quaia M, Minoprio A, Turco E, Mazzei F. 2013. Loss of MUTYH function in human cells leads to accumulation of oxidative damage and genetic instability. Oncogene 32(38):4500.

Saad H, Gallardo F, Dalvai M, Tanguy-le-Gac N, Lane D, Bystricky K. 2014. DNA dynamics during early double-strand break processing revealed by non-intrusive imaging of living cells. PLoS Genet 10(3):e1004187.

Sage E and Harrison L. 2011. Clustered DNA lesion repair in eukaryotes: Relevance to mutagenesis and cell survival. Mutation Research/Fundamental and Molecular Mechanisms of Mutagenesis 711(1–2):123-33.

Santivasi WL and Xia F. 2014. Ionizing radiation-induced DNA damage, response, and repair. Antioxidants & Redox Signaling 21(2):251-9.

Savitsky K, Bar-Shira A, Gilad S, Rotman G, Ziv Y, Vanagaite L, Tagle D, Smith S, Uziel T, Sfez S, et al. 1995a. A single ataxia telangiectasia gene with a product similar to PI-3 kinase. Science 268(5218):1749-53.

Savitsky K, Sfez S, Tagle DA, Ziv Y, Sartiel A, Collins FS, Shiloh Y, Rotman G. 1995b. The complete sequence of the coding region of the ATM gene reveals similarity to cell cycle regulators in different species. Human Molecular Genetics 4(11):2025-32.

Scherthan H and Adelfalk C. 2011. Live cell imaging of meiotic chromosome dynamics in yeast. DNA Recombination: Methods and Protocols :537-48.

Schindelin J, Arganda-Carreras I, Frise E, Kaynig V, Longair M, Pietzsch T, Preibisch S, Rueden C, Saalfeld S, Schmid B. 2012. Fiji: An open-source platform for biological-image analysis. Nature Methods 9(7):676-82.

Schneider CA, Rasband WS, Eliceiri KW. 2012. NIH image to ImageJ: 25 years of image analysis. Nature Methods 9(7):671-5.

Schultz LB, Chehab NH, Malikzay A, Halazonetis TD. 2000. P53 binding protein 1 (53bp1) is an early participant in the cellular response to DNA double-strand breaks. The Journal of Cell Biology 151(7):1381-90.

Seeber A and Gasser SM. 2017. Chromatin organization and dynamics in double-strand break repair. Curr Opin Genet Dev 43:9-16.

Seeber A, Dion V, Gasser SM. 2013. Checkpoint kinases and the INO80 nucleosome remodeling complex enhance global chromatin mobility in response to DNA damage. Genes Dev 27(18):1999-2008.

Segal E and Widom J. 2009. What controls nucleosome positions? Trends in Genetics 25(8):335-43.

Semenenko VA and Stewart RD. 2004. A fast monte carlo algorithm to simulate the spectrum of DNA damages formed by ionizing radiation. Radiat Res 161(4):451-7.

Shakeri Manesh S, Sangsuwan T, Pour Khavari A, Fotouhi A, Emami SN, Haghdoost S. 2017. MTH1, an 8-oxo-2′-deoxyguanosine triphosphatase, and MYH, a DNA glycosylase, cooperate to inhibit mutations induced by chronic exposure to oxidative stress of ionising radiation. Mutagenesis 32(3):389-96.

Shakeri Manesh S, Deperas-Kaminska M, Fotouhi A, Sangsuwan T, Harms-Ringdahl M, Wojcik A, Haghdoost S. 2014. Mutations and chromosomal aberrations in hMTH1-transfected and non-transfected TK6 cells after exposure to low dose rates of gamma radiation. Radiat Environ Biophys 53(2):417-25.

Shilatifard A. 2008. Molecular implementation and physiological roles for histone H3 lysine 4 (H3K4) methylation. Curr Opin Cell Biol 20(3):341-8.

Shiloh Y. 2001. ATM and ATR: Networking cellular responses to DNA damage. Curr Opin Genet Dev 11(1):71-7.

Shimada K and Gasser SM. 2017. A game of musical chairs: Pro- and anti-resection factors compete for TOPBP1 binding after DNA damage. J Cell Biol 216(3):535-7.

Shogren-Knaak M, Ishii H, Sun JM, Pazin MJ, Davie JR, Peterson CL. 2006. Histone H4-K16 acetylation controls chromatin structure and protein interactions. Science 311(5762):844-7.

Sibony D, Horowitz YS, Oster L, Wojcik A, Sollazzo A. 2014. Combined measurement of dose and α/γ radiation-field-components using the shape of composite peak 5 in the glow curve of LiF:Mg,ti. Radiat Measur 71:86-9.

Sihver L., Kodaira S., Ambrožová I., Uchihori Y. and Shurshakov V. 2016. Radiation environment onboard spacecraft at LEO and in deep space. Aerospace conference, 2016 IEEEIEEE. 1 p.

Siranart N, Blakely EA, Cheng A, Handa N, Sachs RK. 2016. Mixed beam murine harderian gland tumorigenesis: Predicted dose-effect relationships if neither synergism nor antagonism occurs. Radiat Res 186(6):577-91.

Skopek TR, Liber HL, Penman BW, Thilly WG. 1978. Isolation of a human lymphoblastoid line heterozygous at the thymidine kinase locus: Possibility for a rapid human cell mutation assay. Biochem Biophys Res Commun 84(2):411-6.

Slupska MM, Luther WM, Chiang JH, Yang H, Miller JH. 1999. Functional expression of hMYH, a human homolog of the escherichia coli MutY protein. J Bacteriol 181(19):6210-3.

Sonoda E, Hochegger H, Saberi A, Taniguchi Y, Takeda S. 2006. Differential usage of non-homologous end-joining and homologous recombination in double strand break repair. DNA Repair 5(9):1021-9.

Sørensen BS, Overgaard J, Bassler N. 2011. In vitro RBE-LET dependence for multiple particle types. Acta Oncol 50(6):757-62.

Staaf E, Brehwens K, Haghdoost S, Pachnerova-Brabcova K, Czub J, Braziewicz J, Nievaart S, Wojcik A. 2012a. Characterisation of a setup for mixed beam exposures of cells to 241Am alpha particles and X-rays. Radiat Prot Dosimetry 151(3):570-9.

Staaf E, Deperas-Kaminska M, Brehwens K, Haghdoost S, Czub J, Wojcik A. 2013. Complex aberrations in lymphocytes exposed to mixed beams of 241Am alpha particles and X-rays. Mutation Research/Genetic Toxicology and Environmental Mutagenesis 756(1–2):95-100.

Staaf E, Brehwens K, Haghdoost S, Nievaart S, Pachnerova-Brabcova K, Czub J, Braziewicz J, Wojcik A. 2012b. Micronuclei in human peripheral blood lymphocytes exposed to mixed beams of X-rays and alpha particles. Radiat Environ Biophys 51(3):283-93.

Stevens TJ, Lando D, Basu S, Atkinson LP, Cao Y, Lee SF, Leeb M, Wohlfahrt KJ, Boucher W, O'Shaughnessy-Kirwan A. 2017. 3D structures of individual mammalian genomes studied by single-cell hi-C. Nature .

Sung P. 1997. Function of yeast Rad52 protein as a mediator between replication protein A and the Rad51 recombinase. Journal of Biological Chemistry 272(45):28194-7.

Sutherland BM, Bennett PV, Sidorkina O, Laval J. 2000. Clustered damages and total lesions induced in DNA by ionizing radiation: Oxidized bases and strand breaks. Biochemistry (N Y) 39(27):8026-31.

Sutherland BM, Bennett PV, Schenk H, Sidorkina O, Laval J, Trunk J, Monteleone D, Sutherland J. 2001. Clustered DNA damages induced by high and low LET radiation, including heavy ions. Phys Med 17 Suppl 1:202-4.

Sutherland BM, Bennett PV, Sutherland JC, Laval J. 2002. Clustered DNA damages induced by X rays in human cells. Radiat Res 157(6):611-6.

Svoboda P and Harms-Ringdahl M. 2005. Influence of chromatin structure and radical scavengers on yields of radiation-induced 8-oxo-dG and DNA strand breaks in cellular model systems. Radiat Res 164(3):303-11.

Symonds H, Krall L, Remington L, Saenz-Robles M, Lowe S, Jacks T, Van Dyke T. 1994. p53-dependent apoptosis suppresses tumor growth and progression in vivo. Cell 78(4):703-11.

Szostak JW, Orr-Weaver TL, Rothstein RJ, Stahl FW. 1983. The double-strand-break repair model for recombination. Cell 33(1):25-35.

Takai H, Smogorzewska A, de Lange T. 2003. DNA damage foci at dysfunctional telomeres. Current Biology 13(17):1549-56.

Takata H, Hanafusa T, Mori T, Shimura M, Iida Y, Ishikawa K, Yoshikawa K, Yoshikawa Y, Maeshima K. 2013. Chromatin compaction protects genomic DNA from radiation damage. PLoS ONE 8(10):e75622.

Terato H, Tanaka R, Nakaarai Y, Nohara T, Doi Y, IWai S, Hirayama R, Furusawa Y, Ide H. 2008. Quantitative analysis of isolated and clustered DNA damage induced by gamma-rays, carbon ion beams, and iron ion beams. J Radiat Res 49(2):133-46.

Tsai CJ, Kim SA, Chu G. 2007. Cernunnos/XLF promotes the ligation of mismatched and noncohesive DNA ends. Proceedings of the National Academy of Sciences 104(19):7851-6.

Tsai-Wu JJ, Liu HF, Lu AL. 1992. Escherichia coli MutY protein has both N-glycosylase and apurinic/apyrimidinic endonuclease activities on A.C and A.G mispairs. Proceedings of the National Academy of Sciences 89(18):8779-83.

Uziel T, Lerenthal Y, Moyal L, Andegeko Y, Mittelman L, Shiloh Y. 2003. Requirement of the MRN complex for ATM activation by DNA damage. Embo J 22(20):5612-21.

Valko M, Leibfritz D, Moncol J, Cronin MT, Mazur M, Telser J. 2007. Free radicals and antioxidants in normal physiological functions and human disease. Int J Biochem Cell Biol 39(1):44-84.

van Loon B and Hübscher U. 2009. An 8-oxo-guanine repair pathway coordinated by MUTYH glycosylase and DNA polymerase λ. Proceedings of the National Academy of Sciences 106(43):18201-6.

Venkatesh P, Panyutin IV, Remeeva E, Neumann RD, Panyutin IG. 2016. Effect of chromatin structure on the extent and distribution of DNA double strand breaks produced by ionizing radiation; comparative study of hESC and differentiated cells lines. International Journal of Molecular Sciences 17(1):58.

Vogiatzi F, Brandt DT, Schneikert J, Fuchs J, Grikscheit K, Wanzel M, Pavlakis E, Charles JP, Timofeev O, Nist A, et al. 2016. Mutant p53 promotes tumor progression and metastasis by the endoplasmic reticulum UDPase ENTPD5. Proc Natl Acad Sci U S A 113(52):E8433-42.

von Sonntag C. 1987. The chemical basis of radiation biology. Taylor & Francis London.

Wade M, Wang YV, Wahl GM. 2010. The p53 orchestra: Mdm2 and mdmx set the tone. Trends Cell Biol 20(5):299-309.

Walker JR, Corpina RA, Goldberg J. 2001. Structure of the ku heterodimer bound to DNA and its implications for double-strand break repair. Nature 412(6847):607-14.

Wang H, Wang L, Erdjument-Bromage H, Vidal M. 2004. Role of histone H2A ubiquitination in polycomb silencing. Nature 431(7010):873.

Ward IM, Reina-San-Martin B, Olaru A, Minn K, Tamada K, Lau JS, Cascalho M, Chen L, Nussenzweig A, Livak F, et al. 2004. 53BP1 is required for class switch recombination. The Journal of Cell Biology 165(4):459-64.

Ward JF. 1994. The complexity of DNA damage: Relevance to biological consequences. Int J Radiat Biol 66(5):427-32.

Ward JF. 1985. Biochemistry of DNA lesions. Radiat Res 104(2):S103-11.

Wardlaw CP, Carr AM, Oliver AW. 2014. TopBP1: A BRCT-scaffold protein functioning in multiple cellular pathways. DNA Repair 22:165-74.

Warters RL and Lyons BW. 1992. Variation in radiation-induced formation of DNA double-strand breaks as a function of chromatin structure. Radiat Res 130(3):309-18.

Weber SC, Spakowitz AJ, Theriot JA. 2012. Nonthermal ATP-dependent fluctuations contribute to the in vivo motion of chromosomal loci. Proceedings of the National Academy of Sciences 109(19):7338-43.

Weber SC, Spakowitz AJ, Theriot JA. 2010a. Bacterial chromosomal loci move subdiffusively through a viscoelastic cytoplasm. Phys Rev Lett 104(23):238102.

Weber SC, Spakowitz AJ, Theriot JA. 2010b. Bacterial chromosomal loci move subdiffusively through a viscoelastic cytoplasm. Phys Rev Lett 104(23):238102.

Weinberg R. 2007. The biology of cancer. Second Edition ed. Garland Publishing Inc.

Weiss M, Elsner M, Kartberg F, Nilsson T. 2004. Anomalous subdiffusion is a measure for cytoplasmic crowding in living cells. Biophys J 87(5):3518-24.

Wilson JW. 2000. Overview of radiation environments and human exposures. Health Phys 79(5):470-94.

Wilson MD, Benlekbir S, Fradet-Turcotte A, Sherker A, Julien J, McEwan A, Noordermeer SM, Sicheri F, Rubinstein JL, Durocher D. 2016. The structural basis of modified nucleosome recognition by 53BP1. Nature 536(7614):100-3.

Wojewódzka M, Kruszewski M, Iwaneñko T, Collins AR, Szumiel I. 1998. Application of the comet assay for monitoring DNA damage in workers exposed to chronic low-dose irradiation: I. strand breakage. Mutation Research/Genetic Toxicology and Environmental Mutagenesis 416(1–2):21-35.

Woods CG and Taylor AMR. 1992. Ataxia telangiectasia in the british isles: The clinical and laboratory features of 70 affected individuals. QJM: An International Journal of Medicine 82(2):169-79.

Xue W, Zender L, Miething C, Dickins RA, Hernando E, Krizhanovsky V, Cordon-Cardo C, Lowe SW. 2007. Senescence and tumour clearance is

triggered by p53 restoration in murine liver carcinomas. Nature 445(7128):656-60.

Yang N, Galick H, Wallace SS. 2004. Attempted base excision repair of ionizing radiation damage in human lymphoblastoid cells produces lethal and mutagenic double strand breaks. DNA Repair 3(10):1323-34.

Zanini A, Durisi E, Fasolo F, Ongaro C, Visca L, Nastasi U, Burn K, Scielzo G, Adler J, Annand J. 2004. Monte carlo simulation of the photoneutron field in linac radiotherapy treatments with different collimation systems. Phys Med Biol 49(4):571.

Zgheib O, Huyen Y, DiTullio Jr RA, Snyder A, Venere M, Stavridi ES, Halazonetis TD. 2005. ATM signaling and 53BP1. Radiotherapy and Oncology 76(2):119-22.

Zhang X, De Silva D, Sun B, Fisher J, Bull RJ, Cotruvo JA, Cummings BS. 2010. Cellular and molecular mechanisms of bromate-induced cytotoxicity in human and rat kidney cells. Toxicology 269(1):13-23.

Zhang Y and Xiong Y. 1999. Mutations in human ARF exon 2 disrupt its nucleolar localization and impair its ability to block nuclear export of MDM2 and p53. Mol Cell 3(5):579-91.

Zhang Y and Reinberg D. 2001. Transcription regulation by histone methylation: Interplay between different covalent modifications of the core histone tails. Genes Dev 15(18):2343-60.

Zhou G, Bennett PV, Cutter NC, Sutherland BM. 2006. Proton-HZE-particle sequential dual-beam exposures increase anchorage-independent growth frequencies in primary human fibroblasts. Radiat Res 166(3):488-94.

Zimmermann M and de Lange T. 2014. 53BP1: Pro choice in DNA repair. Trends Cell Biol 24(2):108-17.